Published in final edited form as:

J Immunol. 2020 December 15; 205(12): 3263–3276. doi:10.4049/jimmunol.1900464.

T-B Lymphocyte Interactions Promote Type 1 Diabetes Independently of SLAM-Associated Protein

Rachel H. Bonami[†,‡,*], **Lindsay E. Nyhoff**[‡,¶], **Dudley H. McNitt**[†], **Chrys Hulbert**[†], **Jamie L. Felton**[§], **Peggy Kendall**[‡,¶], **James W. Thomas**[†,‡,*]

[†]Department of Medicine, Division of Rheumatology and Immunology, Pulmonary, and Critical Care, Vanderbilt University Medical Center, Nashville, TN 37232

[‡]Department of Pathology, Microbiology and Immunology, Pulmonary, and Critical Care, Vanderbilt University Medical Center, Nashville, TN 37232

[§]Department of Pediatrics, Division of Pediatric Endocrinology and Diabetes, Pulmonary, and Critical Care, Vanderbilt University Medical Center, Nashville, TN 37232

[¶]Department of Medicine, Division of Allergy, Pulmonary, and Critical Care, Vanderbilt University Medical Center, Nashville, TN 37232

Abstract

Signaling lymphocytic activation molecule-associated protein (SAP), a critical intracellular signaling molecule for T-B lymphocyte interactions, drives T follicular helper (Tfh) cell development in germinal centers (GCs). High-affinity islet autoantibodies predict type 1 diabetes (T1D) but do not cause beta cell destruction. This paradox intimates Tfh cells as key pathologic effectors, consistent with an observed Tfh signature in T1D. To understand how fully developed Tfh (GC Tfh) contribute to different autoimmune processes, we investigated the role of SAP in T1D and autoantibody-mediated arthritis. Whereas spontaneous arthritis depended on SAP in the autoantibody-mediated K/BxN model, organized insulitis and diabetes onset were unabated, despite a blocked anti-insulin vaccine response in *SAP*-deficient non-obese diabetic (NOD) mice. GC Tfh and GC B cell development was blocked by loss of *SAP* in K/BxN mice. In contrast, although GC B cell formation was markedly reduced in *SAP*-deficient NOD mice, T cells with a GC Tfh phenotype were found at disease sites. $CXCR3^{+}$ $CCR6^{-}$ (Tfh1) subset bias was observed among GC Tfh cells infiltrating the pancreas of NOD mice, which was enhanced by loss of *SAP*. NOD T cells override *SAP* requirement to undergo activation and proliferation in response to antigen presentation, demonstrating the potential for productive cognate T-B lymphocyte interactions in T1D-prone mice. We find that SAP is essential when autoantibody-driven immune complexes promote inflammation but is not required for effective organ-specific autoimmune attack. Thus, Tfh induced in classic GC reactions are dispensable for T1D but the autoimmune process in NOD retains pathogenic Tfh without SAP.

[*]Corresponding Authors: James W. Thomas, james.w.thomas@vumc.org and Rachel H. Bonami, rachel.h.bonami@vumc.org, Vanderbilt University Medical Center, Medical Center North T3113, 1161 21st Avenue South, Nashville, TN 37232.

Author Contributions

R.H.B. performed experiments and wrote the manuscript. L.E.N., C.H., D.M., and J.L.F. performed experiments. P.L.K and J.W.T. critically reviewed the manuscript. All authors provided helpful experimental discussion.

Introduction

Autoimmune diseases previously attributed solely to T cells are effectively treated by B lymphocyte elimination, highlighting the critical role of T-B cell interactions in autoimmunity (1). Vaccine studies demonstrate that productive interactions between antigen-specific T and B lymphocytes are central to the development of protective immunity; similar interactions are assumed to mediate autoimmunity. T follicular helper (Tfh) cells drive B cell class switching and antibody responses following infection or T-dependent immunization (2). Signaling lymphocytic activation molecule (SLAM)-associated protein (SAP) is essential in facilitating long-lasting cognate T-B cell interactions necessary for protective immune responses to develop in these settings (3–9). The bulk of work describing the requirements for GC Tfh formation stems from studying infection and vaccine responses, whereas less is known about the molecular governance of Tfh in autoimmunity. In contrast to immune complex-dependent diseases, B lymphocyte-dependent organ-specific autoimmunity can arise independently of autoantibody (10–12). It is unclear whether SAP-supported T-B interactions are necessary to drive such organ-specific autoimmune processes.

T1D is a classic organ-specific autoimmune disease that arises through T cell-mediated attack of insulin-producing beta cells in islets. T cell-mediated attack on islets drives T1D and is dependent on islet autoantigen presentation by B lymphocytes (11–16). Islet autoantibodies predict T1D development but are not thought to act as pathogenic effector molecules (12, 16, 17); rather, they are a biomarker of autoimmune GCs during the disease prodrome. As such, NOD serum transfer does not cause T1D (12). This contrasts with the K/BxN model of autoimmune arthritis, in which serum transfer is sufficient to drive joint pathology in recipients (18). This spontaneous arthritis model is produced through combination of the disease-permissive NOD IA^{g7} MHC class II allele that results in glucose-6-phosphate isomerase (GPI) recognition by the KRN TCR transgene (19). Autoreactive T-B interactions drive GC formation, immune complex deposition, and ultimately joint destruction in K/BxN mice (18, 20). Rituximab (B cell depletion) efficacy in both T1D and RA is attributed to disruption of cognate T-B interactions (1, 21). T1D shares the development of tertiary lymphoid structures and GC formation at the site of autoimmune attack with rheumatoid arthritis (22, 23). High-affinity autoantibodies, a molecular Tfh signature, and increased peripheral blood Tfh in T1D patients point to a role for Tfh in the disease process (17, 24, 25). Furthermore, baseline Tfh subsets predict clinical response to abatacept among individuals with T1D (26). Tfh-like cells are also recognized in the rheumatoid synovium (27). Contributions of Tfh to autoimmune pathology are observed in murine models of both RA and T1D in which the *san* allele of *Roquin*, a RING-type ubiquitin ligase, drives dysregulated Tfh and accelerates both diseases (28, 29). The RA and T1D models therefore exemplify distinct types of autoimmune responses predicted to possess a common Tfh cell dependency.

SAP is required for autoimmune arthritis initiated by an acute event such as when a bolus of antigen is delivered for initiation of collagen-induced arthritis or when GPI-reactive KRN T cells are transferred into IA^{g7}+ recipients (30, 31). Loss of *SAP* also ameliorates features of the autoantibody-mediated disease, systemic lupus erythematosus (SLE) and prevents the overexuberant germinal center responses and GC Tfh that otherwise drive SLE

manifestations in *sanroque* mice (6, 28, 32). It is unclear whether *SAP*-supported T-B interactions are necessary to drive organ-specific autoimmune diseases such as T1D which are B lymphocyte-dependent but not autoantibody-mediated in mice (10–12). The impact of *SAP* on disrupting Tfh development and GC responses was therefore investigated in spontaneous models of T1D and RA. *SAP*-deficient NOD T cells proliferated to cognate antigen stimulation by B cells and acquired the GC Tfh phenotype. The requirement for *SAP* is therefore overridden in the development of the organ-specific autoimmune disease, T1D, but not the systemic immune complex-mediated disease, autoimmune arthritis. These findings suggest that T-B interactions are governed differently based on the context of the immune response. Tfh cells may serve pathologic roles in autoimmune settings even in the absence of classical germinal center reactions. This is an important consideration for the development of immune-targeted therapy in cell-mediated autoimmunity.

Materials and Methods

Animals

SAP-deficient mice on the C57BL/6 background (5, 9) were provided by Dr. Pamela Schwartzberg (National Institutes of Health), bred in our colony, and subsequently backcrossed to the NOD strain. Anti-insulin 125Tg/NOD and $VH125^{SD}$/NOD BCR Tg mice were described previously (33, 34). 8F10/NOD mice (35) were provided by Emil Unanue (Washington University School of Medicine). NOD.Cg-Tg(TcraBDC2.5,TcrbBDC2.5)1Doi/DoiJ (BDC2.5/NOD) and B6.Cg-Tg(TcraTcrb)425Cbn/J (OT-II/C57BL/6) mice were purchased from the Jackson Laboratory. All NOD strains were backcrossed ≥11 generations. $KRN^{+/-}$/C57BL/6 mice (a gift from Dr. Christophe Benoist and Diane Mathis, Harvard Medical School, Boston, MA) were crossed with NOD mice to generate K/BxN mice. All mice were housed under specific pathogen-free conditions. All animal studies were approved by the fully AAALAC-accredited Vanderbilt University IACUC.

Histological assessment and monitoring of disease activity

Insulitis assessment was performed using non-diabetic, female NOD mice. Pancreata were dissected and immediately fixed with neutral buffered formalin for 4–6 h and then incubated overnight in 70% ethanol at room temperature. 5μm sections were cut from paraffin-embedded tissues and stained with H&E. Slide images were acquired using a bright field Aperio ScanScope CS and visualized using ImageScope software (Leica Biosystems). All islets in a section were blind scored (average = 26, min = 9, max = 51). Blood glucose was measured in NOD or $SAP^{-/-}$/NOD mice to confirm symptomatic diabetes onset as described previously (36). Hind paws were isolated from K/BxN mice post-mortem, fixed in 4% paraformaldehyde, decalcified in EDTA, and paraffin embedded. Two blinded observers scored lymphocytic inflammation, cartilage loss, and bone erosion in H&E stained 5 μm sections of the tibiotalar joint. K/BxN and $SAP^{-/y}$/K/BxN mice were monitored weekly for autoimmune arthritis development as previously described (37).

Pancreas sections were acquired as above, deparafinnized, and a Leica Bond-Max IHC stainer was used for all steps besides dehydration, clearing and applying cover slips. Bond Epitope Retrieval Solution 2 (Leica Biosystems) was used for heat-induced antigen retrieval.

Anti-CD3 (M-20, Santa Cruz Biotechnology) and anti-B220 (RA3–6B2, BD Biosciences) antibodies were detected with biotinylated rabbit anti-goat IgG (Vector Laboratories, BA-5000) or biotinylated rabbit anti-rat IgG (Vector Laboratories, BA-4001), respectively, in combination with the Bond Polymer Refine Detection system. Slides were dehydrated, cleared and cover slips were applied and images were acquired and analyzed as above.

Cell isolation, flow cytometry, and antibodies

Cells were isolated from spleens and pancreata as previously described (36). Lymph nodes were macerated in HBSS (Invitrogen Life Technologies) + 10% FBS (HyClone). Cells were subsequently stained for flow cytometry analysis using the following reagents and reactive antibodies: 7-aminoactinomycin D (7-AAD), B220 (6B2), BCL-6 (K112–91), CCR6 (140706), CD11b (M1/70), CD11c (HL3), CD4 (RM4–5), CD44 (IM7), CD69 (H1.2F3), CD95/FAS (JO2), CD278/ICOS (C398.4A), CXCR3 (CXCR3–173), CXCR5 (2G8), eFluor Fixable Viability Dye, GL7, IgD (11–26c), IgM^a (DS-1), IgM^b (AF6–78), IgM (μ chain specific), NKG2D (cx5), or PD-1 (J43) (BD Biosciences, eBioscience, ThermoFisher Scientific, or Tonbo Biosciences). Biotinylated human insulin (Sigma-Aldrich) (33) was used to detect insulin-binding specificity. Avidin-fluorochrome conjugates were used to detect biotinylated reagents. Samples were acquired using a BD Biosciences LSR II flow cytometer and data were analyzed using FlowJo software (Tree Star, Inc).

Immunization and ELISA

Preimmune sera were collected and 9–12 week-old NOD or $SAP^{-/y}$/NOD mice were immunized s.c. at the base of the tail with 25 μg insulin B10–23 peptide (Schafer-N) emulsified in CFA. Sera were harvested at 3 weeks following immunization, after which mice were boosted with 10 μg B10–23 insulin emulsified in IFA i.p. Insulin-specific IgM or IgG were measured by ELISA as described (33) with the following modifications. Plates were coated with 1 μg/mL human insulin and incubated with sera diluted 1:100 in 1X PBS overnight at 4°C. Insulin autoantibodies were detected with goat anti-mouse IgG or IgM conjugated to alkaline phosphatase (Southern Biotech, 1030–04 and 1020–04). Standard curves were generated using anti-insulin mAb123 (HB-123, ATCC) or mAb301/1F11 (38) antibodies purified from hybridoma supernatants to quantify anti-insulin IgG or IgM antibodies, respectively. Anti-GPI antibody ELISAs were performed as above, but with the following modifications. Plates were coated with 5 μg/mL mouse GPI (Cloud-Clone Corp.) in 1X PBS overnight at 4°C and blocked and washed with 1X PBS/1% BSA. Sera diluted 1:1000 were incubated overnight at 4°C. Bound antibody was detected as above.

ELISpot assay

ELISpot assays to detect IFN-γ were performed as previously described (39). In brief, 96-well filter plates (Millipore) were coated with anti-mouse IFN-γ Ab overnight at 4°C (eBioscience, clone AN-18). Wells were washed and blocked with complete media. Splenocytes were freshly isolated as above and plated at 1×10^6 cells per well with or without 10μM human insulin (Sigma-Aldrich) in complete RPMI 1640 [10% FBS (HyClone), non-essential amino acids, HEPES, sodium pyruvate, penicillin/streptomycin, L-Glutamine, 2×10^5 M 2-ME (Invitrogen)]. Cells were cultured for 72 hours at 37°C in 5% CO_2. After incubation, plates were washed and incubated with biotinylated anti-mouse IFN-

γ Ab (eBioscience, clone R4–6A2). Wells were washed and incubated with horseradish peroxidase (HRP)-conjugated streptavidin (BD Biosciences). After washing, 3-Amino-9-ethylcarbazole (AEC) substrate solution (BD Biosciences) was added and wells were monitored for spot development for 4–10 min. Cold, deionized water was used to stop substrate reaction, and plates were dried overnight. Spots were counted using an ImmunoSpot plate reader (Cellular Technology Limited).

In vitro and in vivo T cell proliferation assays

Magnetic separation was used as above to purify B cells (>86% purity, < 0.4% contamination by IA^{g7+} $CD11b^+$ or $CD11c^+$ antigen presenting cells) from 125Tg/NOD spleens and $CD4^+$ T cells (> 84% purity) as above from BDC2.5/*SAP*-sufficient or BDC2.5/*SAP*-deficient NOD mice. Purified B cells and T cells were labeled with CellTrace Violet (ThermoFisher Scientific) per the manufacturer's instructions. BDC mimotope peptide was conjugated to pork insulin (Eli Lilly) as previously described (15). 0.25×10^6 *SAP*-sufficient or *SAP*-deficient BDC2.5/NOD T cells and $0.016–0.25 \times 10^6$ 125Tg/NOD B cells were co-cultured in complete RPMI with 100 ng/mL Insulin-BDC mimotope conjugate at 37°C in a CO_2 incubator for 3d. Expression of B220, CD4, CD69, viability, and dilution of the CellTrace Violet dye was assessed in harvested cells by flow cytometry. The cell proliferation tool in Flowjo (version 9.6.4, Tree Star, Inc.) was used to identify the Division Index (average number of divisions per cell, including the undivided population) in $CD4^+$ live lymphocytes.

$CD4^+$ T cells were magnetically purified (>90% purity) from 8F10/$SAP^{+/y}$ or 8F10/$SAP^{-/y}$ NOD mice as above and populations were separately labeled with CellTrace Violet or CellTrace Yellow dye. Cells were washed and resuspended in 1X PBS. Equal numbers of labeled 8F10/$SAP^{+/y}$/NOD and 8F10/$SAP^{-/y}$/NOD $CD4^+$ T cells were combined, and $17–20 \times 10^6$ cells of each genotype were injected i.p. per gender-matched $VH125^{SD}$/NOD recipient. After 7 days, cells were isolated from spleen, pancreatic lymph nodes, and pancreas and T cell proliferation and activation were assessed as above.

Statistics

Standard statistical tests utilized for each experiment are indicated in the corresponding figure legends and significance values were calculated using Prism (GraphPad).

Results

SAP is required for the autoantibody-mediated arthritis to develop in K/BxN mice

K/BxN mice express transgenic T cells that recognize GPI in the context of the NOD MHC class II allele, IA^{g7}, develop spontaneous arthritis due to autoantibody production and immune complex deposition in joints (18–20). Expanded GC Tfh and GC B cell populations are present in draining popliteal lymph nodes in arthritic K/BxN mice (37), consistent with a role for B cells in promoting full GC Tfh differentiation (40). BCL-6 is a lineage-defining transcription factor expressed by GC B cells and GC Tfh cells (41–43), therefore it was included in our GC Tfh identification scheme. Flow cytometry phenotyping showed profound defects in GC Tfh cells ($PD1^{high}$ $BCL6^{high}$ $CXCR5^{high}$) and GC B cells ($GL7^{high}$

FAS^{high}) in arthritis-prone K/BxN mice that lacked *SAP* (Fig. 1A–F). The loss of PD1^{high} BCL6^{high} CXCR5^{high} GC Tfh cells is consistent with a loss of *SAP*-dependent T cell functions (2, 8, 9). We next tested how loss of *SAP* impacted the disease process in the spontaneous K/BxN model of acute autoimmunity. Autoantibody production is a necessary and sufficient driver of immune complex-mediated arthritis (18, 44). As such, we measured serum anti-GPI autoantibody, which was reduced nearly 30-fold in *SAP*$^{-/y}$/K/BxN mice (Fig. 1G). *SAP*$^{-/y}$/K/BxN mice were strongly protected from autoimmune arthritis development, as shown by reductions in clinical scores, paw thickness, tibiotalor joint inflammation, cartilage loss, and bone erosion (Fig. 1H–K). These data show that spontaneous immune complex-mediated arthritis is critically dependent on *SAP* and uphold a role for *SAP* in supporting productive germinal center reactions, Tfh development, and autoantibody production in autoimmune arthritis.

SAP-deficient mice fail to produce GC B cells or insulin autoantibody following T-dependent immunization

Immune responses to autoantigens differ from foreign antigens in that they require breaches in immune tolerance to develop. To test whether *SAP* is required for acute responses to the autoantigen, insulin, we T-dependently immunized NOD and *SAP*$^{-/-}$/NOD mice with the insulin B chain epitope, B10–23 in CFA and boosted with B10–23/IFA (45, 46). T1D incidence is lower in male vs. female NOD mice, thus autoantibody-negative male NOD mice were used to maximize detection of insulin antibody that arose from immunization, rather than spontaneously via T1D autoimmunity. A significantly increased proportion of GC B cells and insulin antibody production was observed 3 weeks following T-dependent immunization of WT/NOD mice, whereas *SAP*$^{-/y}$/NOD mice failed to elicit GC B cell or insulin antibody formation (Fig. 2A–C). These data show that acute, vaccination with a critical insulin autoepitope requires *SAP* for the generation of insulin autoantibodies.

Loss of SAP reduces spontaneous insulin autoantibody production in NOD mice, but insulitis and T1D are preserved

Given the expected role of *SAP* in antibody production (3–6), we measured insulin-specific IgG in female NOD or *SAP*$^{-/-}$/NOD mice. Insulin-specific IgG antibodies were detected in NOD mice but were reduced 6-fold in *SAP*$^{-/-}$/NOD mice (Fig. 3A). Autoantibodies are dispensable for T1D; rather, it is B lymphocyte role as antigen-presenting cells that supports beta cell destruction (10–13, 16). Productive, cognate T-B lymphocyte interactions require *SAP* in classic immune responses (4–7, 9) and spontaneous autoimmune arthritis was disrupted by loss of *SAP* (Fig. 1), thus we predicted that *SAP* might also control autoreactive T-B interactions that lead to lymphocytic infiltration in the pancreas. To investigate the contribution of *SAP* to this cell-mediated autoimmune disease, we assessed progression to diabetes and the severity of islet infiltrates in WT/NOD and *SAP*$^{-/-}$/NOD mice. Contrary to the near absence of autoimmune arthritis observed in *SAP*$^{-/y}$/K/BxN mice (Fig. 1), roughly 50% of *SAP*$^{-/-}$/NOD mice developed diabetes and showed a trend towards lower penetrance, but no significant difference in diabetes incidence compared to WT/NOD (Fig. 3B). Lymphocytic infiltration of islets in the pancreas precedes diabetes onset, therefore we investigated whether differences were observed in this inflammatory process at very early (4 and 6 wks of age), early (8–12 wks), intermediate (13–16 wks), and late (17–

20 wks) pre-diabetic intervals. Insulitis was present in both WT/NOD and *SAP*$^{-/-}$/NOD mice. Detection of insulitis was limited in 4 wk old mice but was readily identified in 6 wk old NOD and *SAP*$^{-/-}$/NOD mice (Fig. 3D–E). As expected, insulitis severity increased with age, but no change in insulitis severity was observed at any of the time points examined (Fig. 3D–E). Fig. 3E shows the typically broad distribution of insulitis severity at each time point across individual mice, in line with the wide range of diabetes onset (Fig. 3B).

T and B lymphocyte infiltration and organization in pancreatic islets is not lost in SAP $^{-/-}$/NOD mice

The pre-diabetic interval in NOD mice is marked by progressive islet infiltration and organization of T and B lymphocytes. Peri-insulitis (lymphocytes surrounding, but not infiltrating the islet) can progress to disorganized lymphocyte infiltration into the islet, which can evolve to organized tertiary lymphoid structures that contain discrete T and B cell zones form (22). The *SAP*-dependence of these structural outcomes of cognate autoreactive T-B interactions was therefore investigated. We did not find quantifiable insulitis present at 4 weeks of age, but at 6 weeks, both T and B lymphocytes were observed to surround and infiltrate islets (Fig. 4A–B). Blind scoring of islets revealed no significant difference in insulitis severity between 6 wk old NOD and *SAP*$^{-/-}$/NOD mice (Fig. 4B). We also assessed late insulitis by comparing the organization of T and B lymphocytes in 17–20 wk old mice. Islets were robustly infiltrated by B and T cells that formed a similar percentage of organized vs. disorganized structures in both groups (Fig. 4C–D). These data show that insulitis, tertiary lymphoid structure formation, and diabetes onset occur in the absence of *SAP* in NOD mice, yet insulin autoantibody production is limited. Thus, cellular interactions necessary for a chronically evolving autoimmune attack can arise despite disruption of a protein that is critical for maintaining T-B interactions in vaccine and infection responses.

T cell activation and IFN-γ production is preserved in SAP-deficient NOD mice

T and B lymphocytes form tertiary lymphoid structures in the pancreas of *SAP*$^{-/-}$/NOD mice (Fig. 4C–D). These data raise the question of whether *SAP* is required for functional responses of autoreactive T cells *in vivo*. Endogenous activation, as indicated by CD69 expression levels, was not different between *SAP*$^{-/-}$ and *SAP*$^{+/+}$ CD4 or CD8 T cells in the pancreas or draining lymph nodes of NOD mice (Fig. 5A–B). IFN-γ is a key inflammatory cytokine in type 1 diabetes and is elicited following insulin stimulation in NOD mice (39, 47, 48). IFN-γ responses are intact in non-autoimmune *SAP*-deficient mice (49), therefore we investigated whether baseline and insulin-driven IFN-γ production was intact in *SAP* $^{-/-}$/NOD mice. IFN-γ production was preserved at baseline and following insulin stimulation in *SAP*$^{-/-}$/NOD splenocytes *in vitro* (Fig. 5C).

Loss of SAP reduces GC B cells but not GC Tfh cell formation in T1D

GC B cells possess enhanced antigen presenting capacity and present unique islet epitopes to T cells to drive immune tolerance breach and differentiation of these cells into GC Tfh in NOD mice (34, 50). GCs form within tertiary lymphoid structures in the pancreas of pre-diabetic NOD mice (22). We therefore investigated the requirement for *SAP* in GC B cell and Tfh cell formation in T1D-prone NOD and *SAP*$^{-/-}$/NOD mice. The frequencies and numbers of GC B cells in the pancreas and draining lymph nodes were reduced in *SAP*

$^{-/-}$/NOD mice in the 8–12 and 13–16 wk-old cohorts that exhibited lower or higher amounts of insulitis, respectively (Fig. 6A–C and Fig. 3). A ten-fold lower frequency of GC B cells formed in the pancreatic draining lymph nodes of *SAP*$^{-/-}$/NOD vs. WT/NOD mice, however a small population of GC B cells formed *SAP*$^{-/-}$/NOD mice which increased during the pre-diabetic interval (Fig. 6B–C). The more modest 10-fold decrease contrasts with the more striking 200-fold decrease in GC B cells cause by *SAP*-deficiency in K/BxN mice (Fig. 1). Thus, autoimmune germinal center reactions are reduced, but not fully eliminated by loss of *SAP* in T1D.

CXCR5-enriched T cells from diabetic mice transfer disease into recipients (24). The exacerbation of Tfh formation by the *sanroque* mutation accelerates diabetes in a hen egg lysozyme TCR transgenic model of T1D (51), further pointing to a pathogenic role of Tfh in T1D. Using the same gating strategy to identify GC Tfh cells as in the K/BxN arthritis model (Fig. 1), we found a population of GC Tfh cells in the pancreatic draining lymph nodes that was expanded in the pancreas (Fig. 7). GC Tfh numbers were unchanged in the pancreas and draining lymph nodes of *SAP*$^{-/-}$/NOD vs. WT/NOD mice sacrificed at intermediate and late time points (Fig. 7). This preservation of GC Tfh cells contrasts the 90-fold robust reduction of GC Tfh cells in *SAP*-deficient K/BxN mice (Fig. 1). These data suggest that classic Tfh formation through germinal centers is not required in T1D, and that Tfh are programmed differently in the chronic autoimmune context of T1D.

GC Tfh cells are biased towards CXCR3$^+$ CCR6$^-$ (Tfh1) cells in the pancreas of NOD mice, which is enhanced by loss of SAP

Tfh1 (CXCR3$^+$ CCR6$^-$) and Tfh17 (CXCR3$^+$ CCR6$^+$) cell subsets have been identified that express IFN-γ and/or IL-17 (52–56). NKG2D expression identifies an ex-T-bet population of IFN-γ-producing Tfh cells in humans (57). CD4$^+$ CD28$^-$ T cells express NKG2D and are elevated in SLE (58). These NKG2D$^+$ CD4 T cells, reported to have cytotoxic activity, kill Tregs in mouse models of SLE (59). Given the Th1/IFN-γ signature in NOD mice and the proposed importance of the Th1/Th17 axis in humans (60, 61), we sought to determine whether GC Tfh bias towards any of these functional subsets was present in the pancreas and draining lymph nodes of pre-diabetic mice, and whether it was changed by loss of *SAP*. Tfh1 and Tfh17 subsets were gated as in Fig. 8A and NKG2D$^+$ GC Tfh cell populations were identified as in Fig. 8B. CXCR3$^+$ CCR6$^-$ (Tfh1) phenotype bias was observed among GC Tfh cells in the pancreas and draining lymph nodes relative to CXCR3$^+$ CCR6$^+$ (Tfh17) or CXCR3$^-$ CCR6$^+$ (Tfh2) phenotypes (Fig. 8C), consistent with the IFN-γ signature in NOD mice (60). The proportion of CXCR3$^+$ CCR6$^-$ (Tfh1) GC Tfh cells was significantly elevated in the pancreas of *SAP*$^{-/-}$/NOD mice relative to WT/NOD, whereas no change was observed in the PLN of the same mice. No significant difference was observed in the frequency or number of CXCR3$^-$ CCR6$^+$ (Tfh2) or CXCR3$^+$ CCR6$^+$ (Tfh17) cells, but Th17 frequency trended higher in *SAP*$^{-/-}$/NOD relative to NOD mice (Fig. 8C–D, pancreatic lymph nodes, 0.73 ± 0.41 vs. 0.31 ± 0.36, $p = 0.15$; pancreas, 1.57 ± 1.14 vs. 0.69 ± 0.48, $p = 0.18$, respectively). A subset of GC Tfh cells in the pancreas and draining lymph nodes were NKG2D$^+$, but *SAP*-deficiency did not alter the frequency or number of this subset (Fig. 8C–D).

Given the transient nature of BCL6 expression and GC Tfh phenotype, we also examined CXCR3, CCR6, and NKG2D expression on total CD4$^+$ T cells. Total CD4 T cells in the pancreas and draining lymph nodes were also biased towards the CXCR3$^+$ CCR6$^-$ (Th1) phenotype relative to CXCR3$^+$ CCR6$^+$ (Th17) or CXCR3$^-$ CCR6$^+$ (Th2) phenotypes, but skewing was less striking than what was observed among GC Tfh cells (Sup. Fig. 1). CXCR3$^+$ CCR6$^+$ (Th17) cells accounted for a low percentage of total CD4$^+$ T cells (< 0.2%) but were significantly elevated in the pancreatic draining lymph nodes (but not pancreas) of *SAP*$^{-/-}$/NOD (Sup. Fig. 1A). A subset of total CD4 T cells were NKG2D$^+$, as observed in GC Tfh cells. Overall, these data suggest Th1/Tfh1 bias, while more pronounced among *SAP*$^{-/-}$/NOD GC Tfh infiltrating the pancreas, is not restricted to this GC Tfh cells; rather this programming, along with Th17 bias, is also observed among total CD4 T cells in *SAP*$^{-/-}$/NOD mice.

SAP-deficiency does not impair T cell activation and proliferation in response to cognate antigen presentation by B cells

The critical role that cognate T-B interactions play in T1D is highlighted by the requirement for antigen presentation by islet-reactive B cells to cognate T cells (10–15). To address whether the requirement for *SAP* may be relaxed for T-B cell interactions in the setting of type 1 diabetes, the activation and proliferation potential of *SAP*-sufficient or *SAP*-deficient autoreactive CD4 T cells was assessed in response to B cell antigen presentation. Anti-chromogranin BDC2.5 T cells were co-cultured with anti-insulin NOD B cells (125Tg/NOD) that present insulin-conjugated BDC mimotope and robust CD4$^+$ T cell activation and proliferation was observed in the presence of cognate antigen (Fig. 9). *SAP* deficiency did not alter the frequency of activated CD4$^+$ T cells, even with increased competition due to a reduced number of B cells (Fig. 9B). Furthermore, no proliferative difference was observed in *SAP*-sufficient vs. *SAP*-deficient T cells, even at suboptimal T:B cell ratios (Fig. 9C). Consistent with maintained disease activity, these data show that *SAP* is not necessary for B lymphocyte-induced activation and proliferation of diabetogenic T cells.

Anti-insulin T cells traffic to the pancreas and draining lymph nodes, undergo activation, and proliferate in the absence of SAP

To directly study the responses of insulin-specific lymphocytes (36), we used anti-insulin TCR (8F10) and BCR (VH125^{SD}/NOD) models in which the majority of CD4 T cells or 1–2% of B cells recognize insulin, respectively (34). We distinctly labeled and tracked *SAP*$^{+/y}$ and *SAP*$^{-/y}$ anti-insulin 8F10 CD4$^+$ cells in the same pre-diabetic VH125^{SD}/NOD recipient to eliminate differences in the inflammatory cytokine milieu or disease state. Transferred cells were identified in the spleens, pancreatic draining lymph nodes, and pancreas of VH125^{SD}/NOD recipients (Fig. 10A and data not shown). Whereas all transferred cells expressed CD4 in the spleen and pancreatic draining lymph nodes, a large proportion of labeled cells expressed little if any CD4 on the cell surface in the pancreas (data not shown). A similar phenomenon occurs in chronically stimulated CD4 T cells (62, 63). We therefore identified labeled cells among live lymphocytes to detect this population of highly-activated T cells. The number of *SAP*$^{+/y}$ versus *SAP*$^{-/y}$ transferred T cells recovered was not significantly different in any of the interrogated organs (Fig. 10B). The frequency of divided, transferred T cells was increased in the pancreatic draining lymph nodes and pancreas

relative to the spleen, but was equivalent among *SAP*$^{-/y}$ versus *SAP*$^{+/y}$ transferred T cells in each of the harvested organs (Fig. 10C). CD69 expression was also similar among co-transferred cells (Fig. 10D). These data indicate that autoreactive T lymphocytes can traffic to the pancreatic draining lymph nodes and pancreas, become activated, and undergo proliferation despite lack of *SAP*. Overall, these data point to a surprising *SAP*-independence of autoimmune T cells that drive cell-mediated autoimmunity in T1D.

Discussion

SAP deficiency was employed in this study to investigate how altered T-B cell interactions impact GC Tfh cell, GC B cell, and T1D development. SAP function in T cells is necessary to promote interactions with cognate B lymphocytes that support germinal centers and protective immune responses (4, 8, 9). As B lymphocytes act as essential antigen-presenting cells in T1D (11–16), we anticipated *SAP* ablation would disrupt the critical T-B cell interactions that drive islet attack. Diabetes onset however persisted in *SAP*-deficient NOD mice (Fig. 3), suggesting that the nature of how T-B cell interactions promote T1D is different from those which drive classic, protective immune responses.

Autoimmune arthritis protection is observed in K/BxN mice (Fig. 1), confirming the requirement for SAP in T-dependent autoantibody production. The limited breakthrough in GC formation and autoantibody production in *SAP*-deficient NOD but not K/BxN models of autoimmunity implies that certain settings of chronic autoimmunity alter immune response dependence on *SAP*. The K/BxN RA model involves robust immune responses typical of immunization or infection and diverges from the “smoldering fire” of low but persistent autoantigen stimulation that drives T1D. Symptomatic disease is often observed as early as 3–4 weeks of age in K/BxN mice, whereas it typically arises after 12 weeks of age and may arise beyond 30 wks of age in NOD mice. Furthermore, whereas ubiquitously-expressed GPI is primarily targeted in K/BxN mice due to TCR repertoire restriction to this specificity, multiple beta cell autoantigens that are more regionally restricted are targeted by a polyclonal T cell repertoire in T1D.

IFN-γ is a key inflammatory cytokine that is elevated in T1D, but it is not upregulated in synovial tissue or fluid in RA (47, 48, 64). *SAP*-deficient CD4 T cells of LCMV-infected mice show Th1 skewing (5, 49). Consistent with preserved Th1 responses, *SAP*-deficiency does not disrupt IFN-γ elicited through T cell stimulation or chronic viral infection (5, 65). We have shown previously that splenocytes harvested from anti-insulin BCR transgenic NOD mice that develop accelerated diabetes produce IFN-γ at baseline and following insulin stimulation, and that T cells are a source of this cytokine (39, 66). IFN-γ responses are preserved in *SAP*$^{-/-}$/NOD mice (Fig. 5) and may thus be facilitating productive T-B interactions in organ-specific autoimmune disease independently of SAP. IFN-γ supports spontaneous GC formation in autoimmunity (67). GCs form within tertiary lymphoid structures in the pancreas of NOD mice (22), thus retention of IFN-γ responses may help to explain the preservation of the small numbers of GC B cells observed in NOD mice. We find that T1D occurs despite markedly reduced autoimmune GC responses and insulin autoantibody production in *SAP*-deficient NOD mice (Fig. 3 and 6). This suggests that fully-developed germinal center reactions are not essential for T1D to develop. Unlike

conventional B lymphocytes, GC B cells present distinct pathogenic insulin epitopes required to drive proliferation of cognate T cells (34). As the rate of diabetes onset levels off with age in *SAP*$^{-/-}$/NOD mice, we speculate that SAP may facilitate epitope spread through support of GCs. Thus, GC formation in the pancreas may represent a more terminal stage in the disease process that occurs after substantial beta cell destruction is already underway.

Subsets of GC Tfh cells contribute differently to protective immune responses in humans; Tfh2 (CXCR3^{-} CCR6^{-}) and Tfh17 (CXCR3^{+} CCR6^{+}) subsets stimulate naïve B cells to differentiate into antibody-secreting cells whereas Tfh1 cells (CXCR3^{+} CCR6^{-}) do not (52–55). Several autoimmune diseases show bias towards Tfh2 and Tfh17 over Tfh1 cells, including SLE, Sjögren's syndrome, autoimmune thyroid disease, and multiple sclerosis, which may reflect the pathologic contributions of autoantibodies in these diseases (68). In contrast, no bias was observed in the peripheral blood of T1D patients relative to healthy donors (24). Autoantibodies are not considered to be pathogenic effector molecules in T1D; rather, B cells present autoantigen to drive T cell-mediated islet attack (12, 13, 15), thus Tfh2 or Tfh17 bias may not be required. Investigation of GC Tfh subset bias in the NOD mouse model of T1D revealed a Tfh1 (CXCR3^{+} CCR6^{-}) cell bias in both the pancreas and draining lymph nodes relative to other Tfh subsets (Fig. 8). This bias was also observed among total CD4^{+} T cells in the pancreas (Sup. Fig. 1) and is thus not dependent on GC Tfh programming. Whereas a trend towards increased Tfh17 cells (CXCR3^{+} CCR6^{+}) was observed among GC Tfh cells, a significant increase in Th17 cells among CD4^{+} T cells was observed in the pancreatic draining lymph nodes of *SAP*$^{-/-}$/NOD mice.

CXCR3 is expressed following TCR stimulation (69). This is counteracted by PD-1, which dampens CXCR3 expression to preserve GC Tfh positioning within GCs as opposed to follicles (70). The increased frequency of CXCR3^{+} GC Tfh cells in the pancreas of *SAP*$^{-/-}$/NOD mice would thus be consistent with their reduced ability to localize to GCs. Disrupted CXCL13 signaling scrambles T-B tertiary lymphoid structures and GCs in NOD mice, yet does not block diabetes, further suggesting mature GC structures may not be required for pathogenic T-B interactions necessary to drive T1D (71). T-bet is a transcription factor that classically marks Th1 cells that secrete IFN-γ. NKG2D^{+} CD4+ T cells were reported in humans to be ex-T-bet^{+} cells that have cytotoxic activity (57, 59). Roughly 10% of GC Tfh cells were NKG2D^{+}, further emphasizing the Th1 axis in NOD mice.

SAP-deficient NOD T cells proliferate *in vitro* following co-culture with cognate B cells (Fig. 9). The significance of this *SAP*-independent T cell/B cell interaction *in vitro* is confirmed *in vivo* by demonstrating that transferred *SAP*-deficient anti-insulin T cells traffic to the pancreas and draining lymph nodes and proliferate. We hypothesize molecular control of cognate T and B cell adhesion is altered in NOD mice to increase the likelihood of productive, pathogenic interactions by rare autoreactive T and B cell clones and explain their *SAP*-independence. SAP binds to SLAM-family receptors (SLAMFR), which include SLAM (SLAMF1), CD48 (SLAMF2), Ly9 (SLAMF3), 2B4 (SLAMF4), CD84 (SLAMF5), Ly108 (SLAMF6), and CRACC (SLAMF7). Analysis using the Wellcome Trust Sanger Institute Mouse Genomes Project - Query SNPs, indels or SVs tool (https://www.sanger.ac.uk/sanger/Mouse_SnpViewer/rel-1505) shows that all of these SLAMFR are polymorphic between non-autoimmune and autoimmune mouse strains (not shown). Of

note, many of the NOD SLAMFR polymorphisms are found in the genetic interval that promotes autoimmunity in the B6.*Sle1b* model of SLE and are confirmed or proposed to impart functional consequences, including CD48, Ly9, 2B4, CD84, Ly108, and CRACC (72, 73).

Several Ly108 isoforms identified in various strains of mice have different signaling potential, including Ly108–1, Ly108–2, and Ly108-H1. Ly108–1 signals more strongly than the Ly108–2 isoform in T cells (74), whereas Ly108-H1 signals little if at all in response to TCR stimulation (75). Expression of Ly108–1 is increased in NOD vs. B6 T cells and is proposed to act as a pathogenic isoform; in contrast, Ly108-H1 is present in B6 but not autoimmune NOD or B6.*Sle1b* mice (76). Introduction of Ly108-H1 into B6.*Sle1b* mice diminished T cell-dependent autoimmunity (76). The “protective” Ly108-H1 isoform is proposed to act as a decoy and limit the positive signaling through Ly108–1 and Ly108–2 isoforms in T cells by competing for SLAMFR engagement provided by cognate cells, such as B cells (75). We hypothesize that *SAP*-deficient NOD T cells retain potential to interact productively with cognate, autoreactive B cells because they lack the protective Ly108-H1 isoform and thus the negative regulation that it provides. Examination of the contribution of individual polymorphic SLAMFR to facilitate T-B interactions in the absence of *SAP* in the context of autoimmunity may thus elucidate new targets to disrupt autoreactive T-B cognate interactions that precede autoimmune disease. Overall, these data suggest the role for SAP in promoting such interactions is context dependent and the requirement for SAP in facilitating B cell stimulation of T cell proliferation is overridden in certain settings of autoimmunity.

SAP is not necessary for development of primary immune responses in the setting of infection (4). It is thus possible that T1D liability is supported by a primary immune response, rather than requiring classic germinal selection of high-affinity T and B cell clones. In line with this, we find that efficient GC responses are not required for T1D, consistent with the long-held view that autoantibodies are not necessary pathogenic mediators for this disease process. Rather, B cells primarily drive T1D autoimmunity through antigen presentation (11–16). *SAP*-deficient CD8 T cells show impaired activation-induced cell death (77), thus this key pathogenic effector population is presumably less restrained in $SAP^{-/-}$/NOD mice. As our data show that cognate B cells drive $CD4^+$ T cell proliferation despite loss of *SAP*, we assume B cell antigen presentation and downstream activation of cytotoxic $CD8^+$ T cells persists to drive T1D in *SAP*-deficient NOD mice.

SAP is required for Tfh cell formation when antigen is limiting and presentation primarily occurs by B cells, but not when antigen is plentiful and dendritic cell presentation of antigen occurs (78). We find that GC Tfh-phenotype CD4 T cells develop in the NOD model of T1D in the absence of *SAP*, yet their functional capability is presumed to be impaired considering the decreased GC B cell development and reduced insulin autoantibody production. Tfh and Th1 cells initially induce *Il21* and *Bcl6* (79). A lower percentage of non-Tfh ($PD\text{-}1^{low}$ $BCL6^{low}$) cells was observed in the pancreas (Fig. 7A and not shown), suggesting $CD4^+$ T cells that are initiating the Tfh program are increased at the site of organ-specific attack independently of SAP function. Given the multi-step developmental process by which Tfh emerge, these findings suggest that pathological potential for T1D resides at a stage distinct from functional induction of GCs. In contrast, the pathology mediated by antigen-antibody

complexes in K/BxN autoimmune arthritis requires fully competent Tfh to induce robust GC responses. A better understanding of Tfh developmental stages in NOD may identify targets that can discriminate different pathological processes. These data suggest the development and function of Tfh in T1D do not follow the paradigm derived from vaccine studies. Interventions that target development of Tfh in the setting of protective immunity may therefore be insufficient to ameliorate pathological Tfh in cell-mediated autoimmune diseases such as T1D.

Supplementary Material

Refer to Web version on PubMed Central for supplementary material.

Acknowledgements

We thank Dr. Pamela Schwartzberg and Dr. Jennifer Cannons (National Institutes of Health, Bethesda MD) for providing the *SAP*-deficient C57BL/6 mice and relevant protocols, and Dr. Christophe Benoist and Dr. Diane Mathis (Harvard Medical School, Boston, MA) for providing KRN/C57BL/6 mice. Flow cytometry experiments were performed in the Vanderbilt Medical Center Flow Cytometry Shared Resource. Tissue sections were embedded, cut, and stained by the Vanderbilt Tissue Pathology Shared Resource. Histology sections were imaged using the ScanScope in the Vanderbilt Islet Procurement and Analysis Core. We would like to acknowledge the Vanderbilt Diabetes Research and Training Center and the Vanderbilt Institute for Infection, Immunology, and Inflammation. We thank Bryan Joosse for assistance collecting pancreata for histology studies and Dr. Kristen Hoek for critical manuscript review.

National Institutes of Health Grants R01 AI051448, R01 DK084246, R21 DK091692, and K12 HD043483, T32 AR059039, T32 HD060554, Juvenile Diabetes Research Foundation Grant 3-2013-121, and Veterans' Administration Merit Award I01 BX 002882 supported this work, along with the Vanderbilt Medical Center Flow Cytometry Shared Resource (supported by P30 CA68485, DK058404, P30 EY08126, and G20 RR030956), the Vanderbilt Translational Pathology Shared Resource (supported by 5U24 DK059637), and the Islet Procurement & Analysis Core (supported by DK020593).

Abbreviations:

GC	germinal center
GPI	glucose-6-phosphate isomerase
NOD	non-obese diabetic
SAP	signaling lymphocyte adaptor molecule (SLAM) associated protein
T1D	type 1 diabetes
Tfh	T follicular helper

References

1. Edwards JC, Szczepanski L, Szechinski J, Filipowicz-Sosnowska A, Emery P, Close DR, Stevens RM, and Shaw T. 2004 Efficacy of B-cell-targeted therapy with rituximab in patients with rheumatoid arthritis. N.Engl.J.Med 350: 2572–2581. [PubMed: 15201414]
2. Crotty S 2011 Follicular helper CD4 T cells (TFH). Annu.Rev.Immunol 29: 621–663. [PubMed: 21314428]
3. Al-Alem U, Li C, Forey N, Relouzat F, Fondaneche MC, V Tavtigian S, Wang ZQ, Latour S, and Yin L. 2005 Impaired Ig class switch in mice deficient for the X-linked lymphoproliferative disease gene Sap. Blood 106: 2069–2075. [PubMed: 15941917]

4. Crotty S, Kersh EN, Cannons J, Schwartzberg PL, and Ahmed R. 2003 SAP is required for generating long-term humoral immunity. Nature 421: 282–287. [PubMed: 12529646]
5. Czar MJ, Kersh EN, Mijares LA, Lanier G, Lewis J, Yap G, Chen A, Sher A, Duckett CS, Ahmed R, and Schwartzberg PL. 2001 Altered lymphocyte responses and cytokine production in mice deficient in the X-linked lymphoproliferative disease gene SH2D1A/DSHP/SAP. Proc.Natl.Acad.Sci.U.S.A 98: 7449–7454. [PubMed: 11404475]
6. Hron JD, Caplan L, Gerth AJ, Schwartzberg PL, and Peng SL. 2004 SH2D1A regulates T-dependent humoral autoimmunity. J.Exp.Med 200: 261–266. [PubMed: 15263031]
7. Cannons JL, Yu LJ, Jankovic D, Crotty S, Horai R, Kirby M, Anderson S, Cheever AW, Sher A, and Schwartzberg PL. 2006 SAP regulates T cell-mediated help for humoral immunity by a mechanism distinct from cytokine regulation. J.Exp.Med 203: 1551–1565. [PubMed: 16754717]
8. Cannons JL, Qi H, Lu KT, Dutta M, Gomez-Rodriguez J, Cheng J, Wakeland EK, Germain RN, and Schwartzberg PL. 2010 Optimal germinal center responses require a multistage T cell:B cell adhesion process involving integrins, SLAM-associated protein, and CD84. Immunity 32: 253–265. [PubMed: 20153220]
9. Qi H, Cannons JL, Klauschen F, Schwartzberg PL, and Germain RN. 2008 SAP-controlled T-B cell interactions underlie germinal centre formation. Nature 455: 764–769. [PubMed: 18843362]
10. Acevedo-Suarez CA, Hulbert C, Woodward EJ, and Thomas JW. 2005 Uncoupling of anergy from developmental arrest in anti-insulin B cells supports the development of autoimmune diabetes. J.Immunol 174: 827–833. [PubMed: 15634904]
11. Hulbert C, Riseili B, Rojas M, and Thomas JW. 2001 B cell specificity contributes to the outcome of diabetes in nonobese diabetic mice. J.Immunol 167: 5535–5538. [PubMed: 11698422]
12. Serreze DV, Fleming SA, Chapman HD, Richard SD, Leiter EH, and Tisch RM. 1998 B lymphocytes are critical antigen-presenting cells for the initiation of T cell-mediated autoimmune diabetes in nonobese diabetic mice. J.Immunol 161: 3912–3918. [PubMed: 9780157]
13. Silveira PA, Johnson E, Chapman HD, Bui T, Tisch RM, and V Serreze D. 2002 The preferential ability of B lymphocytes to act as diabetogenic APC in NOD mice depends on expression of self-antigen-specific immunoglobulin receptors. Eur.J.Immunol 32: 3657–3666. [PubMed: 12516557]
14. Noorchashm H, Lieu YK, Noorchashm N, Rostami SY, Greeley SA, Schlachterman A, Song HK, Noto LE, Jevnikar AM, Barker CF, and Naji A. 1999 I-Ag7-mediated antigen presentation by B lymphocytes is critical in overcoming a checkpoint in T cell tolerance to islet beta cells of nonobese diabetic mice. J.Immunol 163: 743–750. [PubMed: 10395666]
15. Kendall PL, Case JB, Sullivan AM, Holderness JS, Wells KS, Liu E, and Thomas JW. 2013 Tolerant anti-insulin B cells are effective APCs. J.Immunol 190: 2519–2526. [PubMed: 23396943]
16. Wong FS, Wen L, Tang M, Ramanathan M, Visintin I, Daugherty J, Hannum LG, Janeway CA Jr., and Shlomchik MJ. 2004 Investigation of the role of B-cells in type 1 diabetes in the NOD mouse. Diabetes 53: 2581–2587. [PubMed: 15448087]
17. Yu L, Robles DT, Abiru N, Kaur P, Rewers M, Kelemen K, and Eisenbarth GS. 2000 Early expression of antiinsulin autoantibodies of humans and the NOD mouse: evidence for early determination of subsequent diabetes. Proc.Natl.Acad.Sci.U.S.A 97: 1701–1706. [PubMed: 10677521]
18. Korganow AS, Ji H, Mangialaio S, Duchatelle V, Pelanda R, Martin T, Degott C, Kikutani H, Rajewsky K, Pasquali JL, Benoist C, and Mathis D. 1999 From systemic T cell self-reactivity to organ-specific autoimmune disease via immunoglobulins. Immunity 10: 451–461. [PubMed: 10229188]
19. Matsumoto I, Staub A, Benoist C, and Mathis D. 1999 Arthritis provoked by linked T and B cell recognition of a glycolytic enzyme. Science 286: 1732–1735. [PubMed: 10576739]
20. Kouskoff V, Korganow AS, Duchatelle V, Degott C, Benoist C, and Mathis D. 1996 Organ-specific disease provoked by systemic autoimmunity. Cell 87: 811–822. [PubMed: 8945509]
21. Pescovitz MD, Greenbaum CJ, Krause-Steinrauf H, Becker DJ, Gitelman SE, Goland R, Gottlieb PA, Marks JB, McGee PF, Moran AM, Raskin P, Rodriguez H, Schatz DA, Wherrett D, Wilson DM, Lachin JM, and Skyler JS. 2009 Rituximab, B-lymphocyte depletion, and preservation of beta-cell function. N.Engl.J.Med 361: 2143–2152. [PubMed: 19940299]

22. Kendall PL, Yu G, Woodward EJ, and Thomas JW. 2007 Tertiary lymphoid structures in the pancreas promote selection of B lymphocytes in autoimmune diabetes. J.Immunol 178: 5643–5651. [PubMed: 17442947]

23. Randen I, Mellbye OJ, Forre O, and Natvig JB. 1995 The identification of germinal centres and follicular dendritic cell networks in rheumatoid synovial tissue. Scand.J.Immunol 41: 481–486. [PubMed: 7725067]

24. Kenefeck R, Wang CJ, Kapadi T, Wardzinski L, Attridge K, Clough LE, Heuts F, Kogimtzis A, Patel S, Rosenthal M, Ono M, Sansom DM, Narendran P, and Walker LS. 2015 Follicular helper T cell signature in type 1 diabetes. J.Clin.Invest 125: 292–303. [PubMed: 25485678]

25. Ferreira RC, Simons HZ, Thompson WS, Cutler AJ, Dopico XC, Smyth DJ, Mashar M, Schuilenburg H, Walker NM, Dunger DB, Wallace C, Todd JA, Wicker LS, and Pekalski ML. 2015 IL-21 production by CD4+ effector T cells and frequency of circulating follicular helper T cells are increased in type 1 diabetes patients. Diabetologia 58: 781–790. [PubMed: 25652388]

26. Edner NM, Heuts F, Thomas N, Wang CJ, Petersone L, Kenefeck R, Kogimtzis A, Ovcinnikovs V, Ross EM, Ntavli E, Elfaki Y, Eichmann M, Baptista R, Ambery P, Jermutus L, Peakman M, Rosenthal M, and Walker LSK. 2020 Follicular helper T cell profiles predict response to costimulation blockade in type 1 diabetes. Nat. Immunol 21: 1244–1255. [PubMed: 32747817]

27. Ma J, Zhu C, Ma B, Tian J, Baidoo SE, Mao C, Wu W, Chen J, Tong J, Yang M, Jiao Z, Xu H, Lu L, and Wang S. 2012 Increased frequency of circulating follicular helper T cells in patients with rheumatoid arthritis. Clin.Dev.Immunol 2012: 827480. [PubMed: 22649468]

28. Linterman MA, Rigby RJ, Wong RK, Yu D, Brink R, Cannons JL, Schwartzberg PL, Cook MC, Walters GD, and Vinuesa CG. 2009 Follicular helper T cells are required for systemic autoimmunity. J.Exp.Med 206: 561–576. [PubMed: 19221396]

29. Ji YR, Kim HJ, Yu DH, Bae KB, Park SJ, Yi JK, Kim N, Park SJ, Oh KB, Hwang SS, Lee S, Kim SH, Kim MO, Lee JW, and Ryoo ZY. 2012 Enforced expression of roquin protein in T cells exacerbates the incidence and severity of experimental arthritis. J. Biol. Chem 287: 42269–42277. [PubMed: 23066015]

30. Zhong MC, and Veillette A. 2013 The adaptor molecule signaling lymphocytic activation molecule (SLAM)-associated protein (SAP) is essential in mechanisms involving the Fyn tyrosine kinase for induction and progression of collagen-induced arthritis. J. Biol. Chem 288: 31423–31436. [PubMed: 24045941]

31. Chevalier N, Macia L, Tan JK, Mason LJ, Robert R, Thorburn AN, Wong CH, Tsai LM, Bourne K, Brink R, Yu D, and Mackay CR. 2016 The Role of Follicular Helper T Cell Molecules and Environmental Influences in Autoantibody Production and Progression to Inflammatory Arthritis in Mice. Arthritis Rheumatol 68: 1026–1038. [PubMed: 26501485]

32. Komori H, Furukawa H, Mori S, Ito MR, Terada M, Zhang MC, Ishii N, Sakuma N, Nose M, and Ono M. 2006 A signal adaptor SLAM-associated protein regulates spontaneous autoimmunity and Fas-dependent lymphoproliferation in MRL-Faslpr lupus mice. J.Immunol 176: 395–400. [PubMed: 16365433]

33. Rojas M, Hulbert C, and Thomas JW. 2001 Anergy and not clonal ignorance determines the fate of B cells that recognize a physiological autoantigen. J.Immunol 166: 3194–3200. [PubMed: 11207272]

34. Wan X, Thomas JW, and Unanue ER. 2016 Class-switched anti-insulin antibodies originate from unconventional antigen presentation in multiple lymphoid sites. J.Exp.Med 213: 967–978. [PubMed: 27139492]

35. Mohan JF, Calderon B, Anderson MS, and Unanue ER. 2013 Pathogenic CD4(+) T cells recognizing an unstable peptide of insulin are directly recruited into islets bypassing local lymph nodes. J.Exp.Med 210: 2403–2414. [PubMed: 24127484]

36. Henry RA, Kendall PL, and Thomas JW. 2012 Autoantigen-Specific B Cell Depletion Overcomes Failed Immune Tolerance in Type 1 Diabetes. Diabetes 61: 2037–2044. [PubMed: 22698916]

37. Nyhoff LE, Barron BL, Johnson EM, Bonami RH, Maseda D, Fensterheim BA, Han W, Blackwell TS, Crofford LJ, and Kendall PL. 2016 Bruton's Tyrosine Kinase Deficiency Inhibits Autoimmune Arthritis in Mice but Fails to Block Immune Complex-Mediated Inflammatory Arthritis. Arthritis Rheumatol 68: 1856–1868. [PubMed: 26945549]

38. Thomas JW, Kralick PM, and Ewulonu UK. 1997 T cell-independent response to Brucella-insulin identifies a preimmune repertoire for insulin. J.Immunol 159: 2334–2341. [PubMed: 9278323]

39. Henry-Bonami RA, Williams JM, Rachakonda AB, Karamali M, Kendall PL, and Thomas JW. 2013 B lymphocyte "original sin" in the bone marrow enhances islet autoreactivity in type 1 diabetes-prone nonobese diabetic mice. J.Immunol 190: 5992–6003. [PubMed: 23677466]

40. Poholek AC, Hansen K, Hernandez SG, Eto D, Chandele A, Weinstein JS, Dong X, Odegard JM, Kaech SM, Dent AL, Crotty S, and Craft J. 2010 In vivo regulation of Bcl6 and T follicular helper cell development. J.Immunol 185: 313–326. [PubMed: 20519643]

41. Johnston RJ, Poholek AC, DiToro D, Yusuf I, Eto D, Barnett B, Dent AL, Craft J, and Crotty S. 2009 Bcl6 and Blimp-1 are reciprocal and antagonistic regulators of T follicular helper cell differentiation. Science 325: 1006–1010. [PubMed: 19608860]

42. Nurieva RI, Chung Y, Martinez GJ, Yang XO, Tanaka S, Matskevitch TD, Wang YH, and Dong C. 2009 Bcl6 mediates the development of T follicular helper cells. Science 325: 1001–1005. [PubMed: 19628815]

43. Yu D, Rao S, Tsai LM, Lee SK, He Y, Sutcliffe EL, Srivastava M, Linterman M, Zheng L, Simpson N, Ellyard JI, Parish IA, Ma CS, Li QJ, Parish CR, Mackay CR, and Vinuesa CG. 2009 The transcriptional repressor Bcl-6 directs T follicular helper cell lineage commitment. Immunity 31: 457–468. [PubMed: 19631565]

44. Maccioni M, Zeder-Lutz G, Huang H, Ebel C, Gerber P, Hergueux J, Marchal P, Duchatelle V, Degott C, van RM, Benoist C, and Mathis D. 2002 Arthritogenic monoclonal antibodies from K/BxN mice. J.Exp.Med 195: 1071–1077. [PubMed: 11956298]

45. Nakayama M, Abiru N, Moriyama H, Babaya N, Liu E, Miao D, Yu L, Wegmann DR, Hutton JC, Elliott JF, and Eisenbarth GS. 2005 Prime role for an insulin epitope in the development of type 1 diabetes in NOD mice. Nature 435: 220–223. [PubMed: 15889095]

46. Daniel D, Gill RG, Schloot N, and Wegmann D. 1995 Epitope specificity, cytokine production profile and diabetogenic activity of insulin-specific T cell clones isolated from NOD mice. Eur.J.Immunol 25: 1056–1062. [PubMed: 7537670]

47. Healey D, Ozegbe P, Arden S, Chandler P, Hutton J, and Cooke A. 1995 In vivo activity and in vitro specificity of CD4+ Th1 and Th2 cells derived from the spleens of diabetic NOD mice. J.Clin.Invest 95: 2979–2985. [PubMed: 7769140]

48. Huang X, Yuang J, Goddard A, Foulis A, James RF, Lernmark A, Pujol-Borrell R, Rabinovitch A, Somoza N, and Stewart TA. 1995 Interferon expression in the pancreases of patients with type I diabetes. Diabetes 44: 658–664. [PubMed: 7540571]

49. Wu C, Nguyen KB, Pien GC, Wang N, Gullo C, Howie D, Sosa MR, Edwards MJ, Borrow P, Satoskar AR, Sharpe AH, Biron CA, and Terhorst C. 2001 SAP controls T cell responses to virus and terminal differentiation of TH2 cells. Nat.Immunol 2: 410–414. [PubMed: 11323694]

50. Glazier KS, Hake SB, Tobin HM, Chadburn A, Schattner EJ, and Denzin LK. 2002 Germinal center B cells regulate their capability to present antigen by modulation of HLA-DO. J.Exp.Med 195: 1063–1069. [PubMed: 11956297]

51. Silva DG, Daley SR, Hogan J, Lee SK, Teh CE, Hu DY, Lam KP, Goodnow CC, and Vinuesa CG. 2011 Anti-islet autoantibodies trigger autoimmune diabetes in the presence of an increased frequency of islet-reactive CD4 T cells. Diabetes 60: 2102–2111. [PubMed: 21788582]

52. Bentebibel SE, Lopez S, Obermoser G, Schmitt N, Mueller C, Harrod C, Flano E, Mejias A, Albrecht RA, Blankenship D, Xu H, Pascual V, Banchereau J, Garcia-Sastre A, Palucka AK, Ramilo O, and Ueno H. 2013 Induction of ICOS+CXCR3+CXCR5+ T H cells correlates with antibody responses to influenza vaccination. Sci. Transl. Med 5: 176ra32–176ra32.

53. Locci M, Havenar-Daughton C, Landais E, Wu J, Kroenke MA, Arlehamn CL, Su LF, Cubas R, Davis MM, Sette A, Haddad EK, Poignard P, and Crotty S. 2013 Human circulating PD-1+CXCR3-CXCR5+ memory Tfh cells are highly functional and correlate with broadly neutralizing HIV antibody responses. Immunity 39: 758–769. [PubMed: 24035365]

54. Boswell KL, Paris R, Boritz E, Ambrozak D, Yamamoto T, Darko S, Wloka K, Wheatley A, Narpala S, McDermott A, Roederer M, Haubrich R, Connors M, Ake J, Douek DC, Kim J, Petrovas C, and Koup RA. 2014 Loss of Circulating CD4 T Cells with B Cell Helper Function during Chronic HIV Infection. PLoS Pathog 10: e1003853. [PubMed: 24497824]

55. Morita R, Schmitt N, Bentebibel SE, Ranganathan R, Bourdery L, Zurawski G, Foucat E, Dullaers M, Oh SK, Sabzghabaei N, Lavecchio EM, Punaro M, Pascual V, Banchereau J, and Ueno H. 2011 Human Blood CXCR5+CD4+ T Cells Are Counterparts of T Follicular Cells and Contain Specific Subsets that Differentially Support Antibody Secretion. Immunity 34: 108–121. [PubMed: 21215658]
56. Powell MD, Read KA, Sreekumar BK, Jones DM, and Oestreich KJ. 2019 IL-12 signaling drives the differentiation and function of a TH1-derived TFH1-like cell population. Sci. Rep 9: 1–12. [PubMed: 30626917]
57. Fang D, Cui K, Mao K, Hu G, Li R, Zheng M, Riteau N, Reiner SL, Sher A, Zhao K, and Zhu J. 2018 Transient T-bet expression functionally specifies a distinct T follicular helper subset. J. Exp. Med 215: 2705–2714. [PubMed: 30232200]
58. Groh V, Brühl A, El-Gabalawy H, Nelson JL, and Spies T. 2003 Stimulation of T cell autoreactivity by anomalous expression of NKG2D and its MIC ligands in rheumatoid arthritis. Proc. Natl. Acad. Sci. U. S. A 100: 9452–9457. [PubMed: 12878725]
59. Yang D, Tian Z, Zhang M, Yang W, Tang J, Wu Y, and Ni B. 2017 NKG2D+CD4+ T Cells Kill Regulatory T Cells in a NKG2D-NKG2D Ligand- Dependent Manner in Systemic Lupus Erythematosus. Sci. Rep 7: 1–13. [PubMed: 28127051]
60. Katz JD, Benoist C, and Mathis D. 1995 T helper cell subsets in insulin-dependent diabetes. Science (80-.) 268: 1185–1188.
61. Reinert-Hartwall L, Honkanen J, Salo HM, Nieminen JK, Luopajärvi K, Härkönen T, Veijola R, Simell O, Ilonen J, Peet A, Tillmann V, Knip M, and Vaarala O. 2015 Th1/Th17 Plasticity Is a Marker of Advanced β Cell Autoimmunity and Impaired Glucose Tolerance in Humans. J. Immunol 194: 68–75. [PubMed: 25480564]
62. Grishkan IV, Ntranos A, Calabresi PA, and Gocke AR. 2013 Helper T cells down-regulate CD4 expression upon chronic stimulation giving rise to double-negative T cells. Cell Immunol 284: 68–74. [PubMed: 23933188]
63. Shivakumar S, Tsokos GC, and Datta SK. 1989 T cell receptor alpha/beta expressing double-negative (CD4-/CD8-) and CD4+ T helper cells in humans augment the production of pathogenic anti-DNA autoantibodies associated with lupus nephritis. J.Immunol 143: 103–112. [PubMed: 2525144]
64. Firestein GS, and Zvaifler NJ. 1987 Peripheral blood and synovial fluid monocyte activation in inflammatory arthritis. II. Low levels of synovial fluid and synovial tissue interferon suggest that gamma-interferon is not the primary macrophage activating factor. Arthritis Rheum 30: 864–871. [PubMed: 3115274]
65. Cannons JL, Yu LJ, Hill B, Mijares LA, Dombroski D, Nichols KE, Antonellis A, Koretzky GA, Gardner K, and Schwartzberg PL. 2004 SAP regulates T(H)2 differentiation and PKC-theta-mediated activation of NF-kappaB1. Immunity 21: 693–706. [PubMed: 15539155]
66. Felton JL, Maseda D, Bonami RH, Hulbert C, and Thomas JW. 2018 Anti-Insulin B Cells Are Poised for Antigen Presentation in Type 1 Diabetes. J.Immunol 201: 861–873. [PubMed: 29950508]
67. Onuora S 2016 Autoimmunity: IFNgamma signals control germinal centre formation. Nat.Rev.Rheumatol 12: 312. [PubMed: 27150665]
68. Kim SJ, Lee K, and Diamond B. 2018 Follicular helper T cells in systemic lupus erythematosus. Front. Immunol 9: 1. [PubMed: 29403488]
69. Nakajima C, Mukai T, Yamaguchi N, Morimoto Y, Park W, Iwasaki M, Gao P, Ono S, Fujiwara H, and Hamaoka T. 2002 Induction of the chemokine receptor CXCR3 on TCR-stimulated T cells: dependence on the release from persistent TCR-triggering and requirement for IFN-γ stimulation. Eur. J. Immunol 32: 1792–1801. [PubMed: 12115663]
70. Shi J, Hou S, Fang Q, Liu X, Liu X, and Qi H. 2018 PD-1 Controls Follicular T Helper Cell Positioning and Function. Immunity 49: 264–274.e4. [PubMed: 30076099]
71. Henry RA, and Kendall PL. 2010 CXCL13 Blockade Disrupts B Lymphocyte Organization in Tertiary Lymphoid Structures without Altering B Cell Receptor Bias or Preventing Diabetes in Nonobese Diabetic Mice. J.Immunol 185: 1460–1465. [PubMed: 20574003]

72. McClive PJ, Baxter AG, and Morahan G. 1994 Genetic polymorphisms of the non-obese diabetic (NOD) mouse. Immunol.Cell Biol 72: 137–142. [PubMed: 7911121]

73. Wandstrat AE, Nguyen C, Limaye N, Chan AY, Subramanian S, Tian XH, Yim YS, Pertsemlidis A, Garner HR Jr., Morel L, and Wakeland EK. 2004 Association of extensive polymorphisms in the SLAM/CD2 gene cluster with murine lupus. Immunity 21: 769–780. [PubMed: 15589166]

74. Zhong MC, and Veillette A. 2008 Control of T lymphocyte signaling by Ly108, a signaling lymphocytic activation molecule family receptor implicated in autoimmunity. J. Biol. Chem 283: 19255–19264. [PubMed: 18482989]

75. Dutta M, and Schwartzberg PL. 2012 Characterization of Ly108 in the thymus: evidence for distinct properties of a novel form of Ly108. J.Immunol 188: 3031–3041. [PubMed: 22393150]

76. Keszei M, Detre C, Rietdijk ST, Munoz P, Romero X, Berger SB, Calpe S, Liao G, Castro W, Julien A, Wu YY, Shin DM, Sancho J, Zubiaur M, Morse HC III, Morel L, Engel P, Wang N, and Terhorst C. 2011 A novel isoform of the Ly108 gene ameliorates murine lupus. J.Exp.Med 208: 811–822. [PubMed: 21422172]

77. Chen G, Tai AK, Lin M, Chang F, Terhorst C, and Huber BT. 2007 Increased proliferation of CD8+ T cells in SAP-deficient mice is associated with impaired activation-induced cell death. Eur.J.Immunol 37: 663–674. [PubMed: 17266174]

78. Deenick EK, Chan A, Ma CS, Gatto D, Schwartzberg PL, Brink R, and Tangye SG. 2010 Follicular helper T cell differentiation requires continuous antigen presentation that is independent of unique B cell signaling. Immunity 33: 241–253. [PubMed: 20691615]

79. Nakayamada S, Kanno Y, Takahashi H, Jankovic D, Lu KT, Johnson TA, Sun HW, Vahedi G, Hakim O, Handon R, Schwartzberg PL, Hager GL, and O'Shea JJ. 2011 Early Th1 cell differentiation is marked by a Tfh cell-like transition. Immunity 35: 919–931. [PubMed: 22195747]

Key Points

- Unlike autoimmune arthritis, insulitis and type 1 diabetes (T1D) develop without *SAP*
- B cell antigen presentation can drive *SAP*-deficient T cell proliferation
- *SAP*$^{-/-}$ NOD mice show intact IFN-γ responses and TFH1 cell pancreatic infiltration

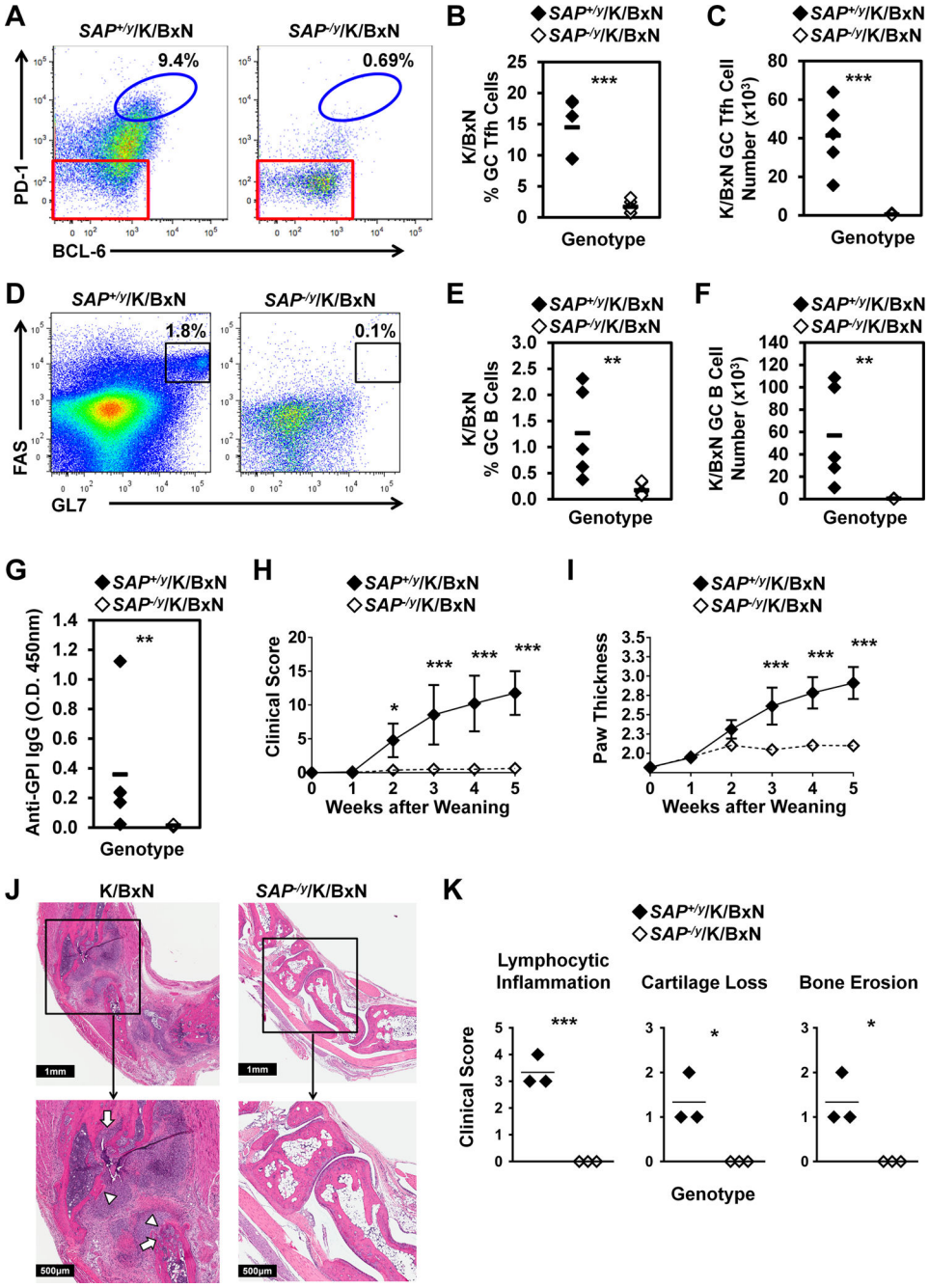

Figure 1. *SAP*-deficient K/BxN mice fail to generate GC Tfh or GC B cells, produce anti-GPI autoantibody, or develop arthritis.

(A-F) *SAP*$^{+/y}$ and *SAP*$^{-/y}$ K/BxN mice were sacrificed at 8–9 wks of age and popliteal lymph nodes were harvested. (A) High levels of BCL-6, PD-1, and CXCR5 (not shown) were used to define GC Tfh cells (blue circle), in contrast to non-Tfh cells (red box). Representative flow cytometry plots are shown. The frequency (B) and number (C) of GC Tfh cells is shown for n ≥ 5 mice per group. (D-F) The frequencies and numbers of GC B cells were assessed as above in the popliteal lymph nodes of *SAP*$^{+/y}$ and *SAP*$^{-/y}$ K/BxN mice. (D) Representative flow cytometry plots show GL7^{high} FAS^{high} GC B cells. The

frequency (E) and number (F) of GC B cells is shown for n ≥ 5 mice per group. (G) Sera were harvested from 8 wk-old n = 5 $SAP^{+/y}$/K/BxN (black) and n = 7 $SAP^{-/y}$/K/BxN (white) mice. Anti-GPI IgG was measured by ELISA as in Methods. (H) $SAP^{+/y}$ (black) or $SAP^{-/y}$ (white) K/BxN mice were scored for arthritis after weaning. (I) Triplicate paw thickness measurements were taken for hind paws and the average is reported. (J) Representative images of H&E stained tibiotalar joint sections. (K) Lymphocytic inflammation (0–4, left panel), cartilage loss (0–2, middle panel), and bone erosion (0–2, right panel) were scored in joint sections from n = 3 mice per group. * $p < 0.05$, ** $p < 0.01$, ** $p < 0.001$, two-tailed t test (panel B-C, E-G, and K), two-way analysis of variance with Sidak correction (panel (H-I).

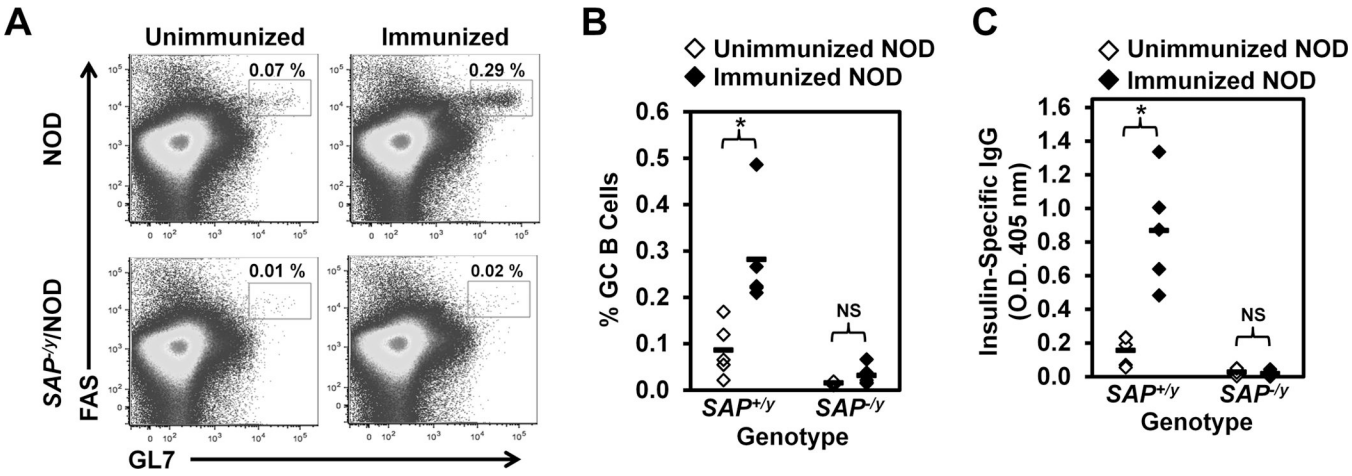

Figure 2. *SAP* is required for T-dependent anti-insulin immune responses in NOD mice.

NOD and $SAP^{-/y}$/NOD mice were immunized with insulin B10–23 peptide in CFA followed by insulin B10–23 peptide/ IFA boost. Spleens were harvested 1 wk after the boost. (A) Representative plots show GC B cells ($GL7^{high}$ FAS^{high}). (B) GC B cell frequency was assessed in n = 4–5 mice per group that were unimmunized (white) or immunized (black). Bars depict averages. (C) Insulin-specific IgG was assessed by ELISA as in Methods in sera harvested 3 wks following immunization with insulin B10–23 peptide in CFA. One $SAP^{+/y}$ mouse was removed from the cohort due to a high level of insulin autoantibody in pre-immune serum. n ≥ 5 mice per group, * $p < 0.05$, Mann-Whitney U test.

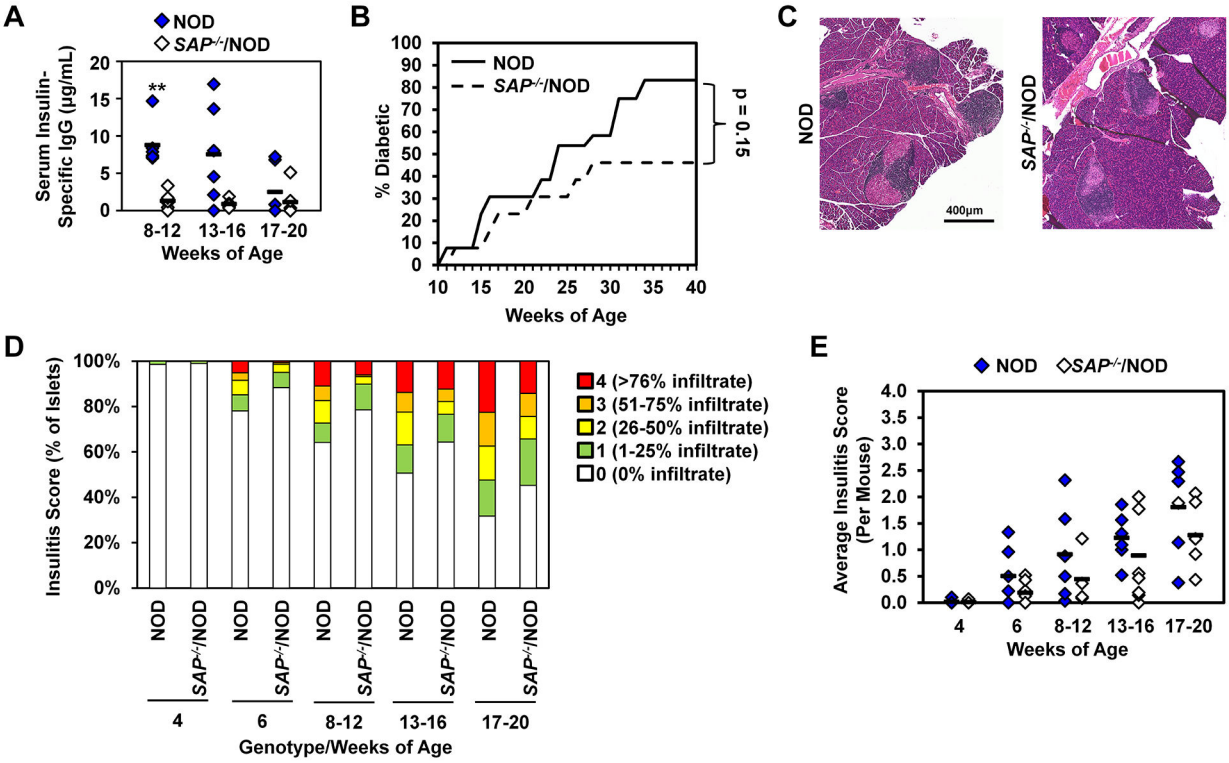

Figure 3. *SAP* is dispensable for insulitis and T1D development but is required for insulin autoantibody production in NOD mice.

NOD and *SAP*$^{-/-}$/NOD sera and pancreata were freshly harvested from female, pre-diabetic mice. (A) ELISA was used to quantify insulin-specific IgG in NOD and *SAP*$^{-/-}$/NOD sera. ** $p < 0.01$, two-tailed t test. (B) Diabetes was monitored in female NOD (solid line) and *SAP*$^{-/-}$/NOD (dashed line) mice starting at 10 wks of age. n = 13 mice per group, p = 0.15, log-rank test. (C-E) NOD and *SAP*$^{-/-}$/NOD pancreata were freshly harvested from female, pre-diabetic mice. (C) Representative H&E stained sections are shown for 17–20wk-old mice. (D-E) All islets were blind scored for n = 4–7 mice per group. (D) Scoring distribution was normalized per mouse to account for variation in the total number of islets scored. The percent of islets with each score is shown. (E) The average insulitis score is plotted for NOD (blue) or *SAP*$^{-/-}$/NOD (white) mice, no significant differences were observed in each age group, two-tailed t test.

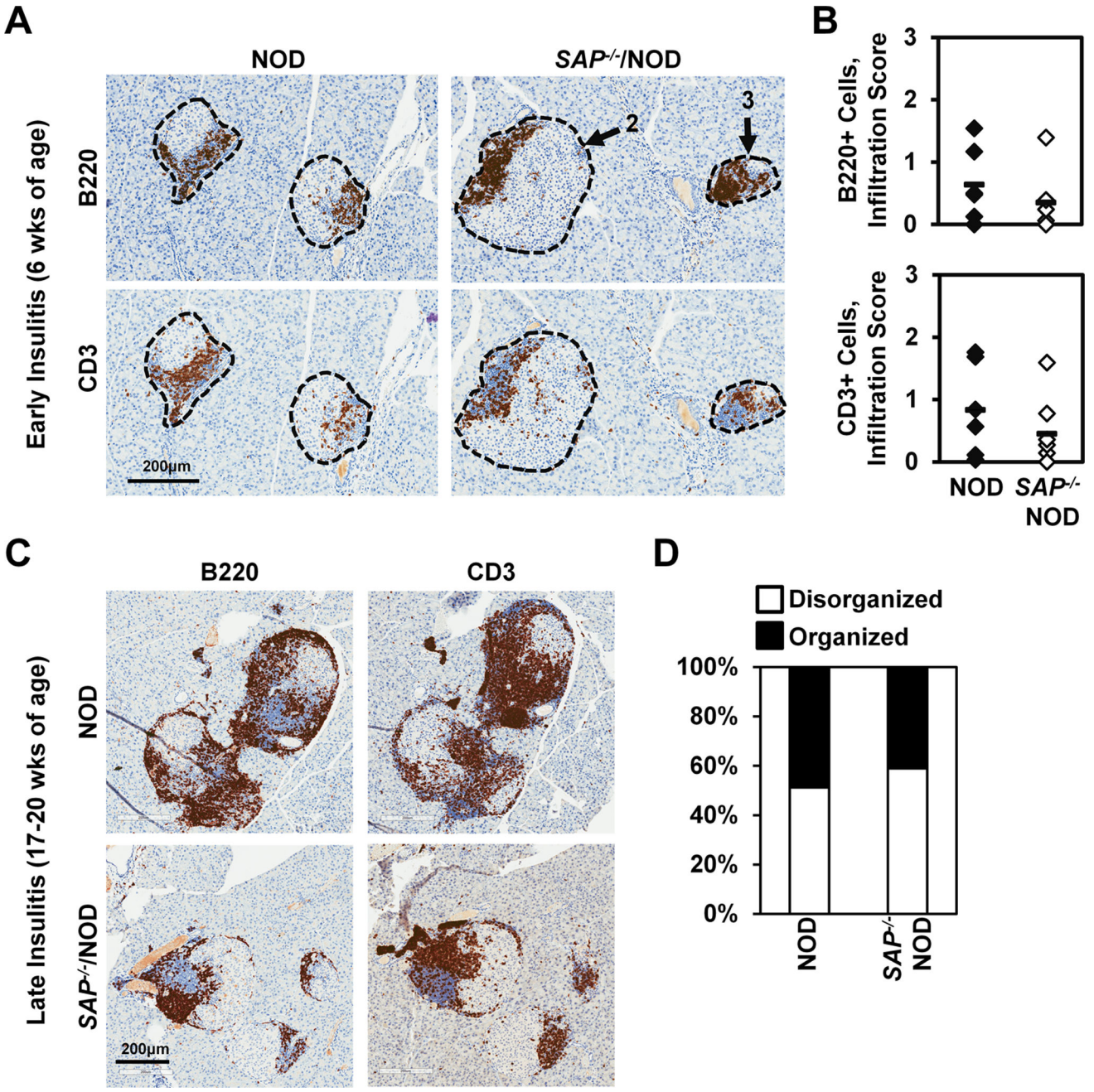

Figure 4. Loss of *SAP* does not prevent early T cell and B cell infiltration or tertiary lymphoid structure formation in NOD mice.

NOD and $SAP^{-/-}$/NOD pancreata were freshly harvested from female, pre-diabetic mice to assess early insulitis (A-B, 6 wk old mice) or late insulitis (C-D, 17–20 wk old mice). Serial sections were stained for B220 or CD3 expression (brown) and counterstained with hematoxylin (blue). (A) Dashed lines indicate islet boundaries, arrows show examples of lymphocyte infiltration scores (0 = no insulitis, 1 = peri-insulitis, 2 = mild lymphocyte infiltration, 3 = moderate/severe lymphocyte infiltration). These scores were assigned separately based on either CD3 or $B220^+$ cells stained in brown. (B) The average lymphocyte infiltration score is shown for $B220^+$ cells (top) or $CD3^+$ cells (bottom), n = 6

individual mice are plotted and bars indicate the overall average score per group. No significant differences were observed, two-tailed t test. (C) Representative images of anti-B220 (left) or anti-CD3 (right) stained serial sections from NOD (top) and *SAP*$^{-/-}$/NOD (bottom) mice. (D) Infiltrated islets were blind scored as Organized (black bars) or Disorganized (white bars) in 17–20 wk old NOD or *SAP*$^{-/-}$/NOD mice. Islets scored as peri-insulitis or no insulitis were excluded from analysis. n = 3 mice per group. p = 0.45, chi-squared test.

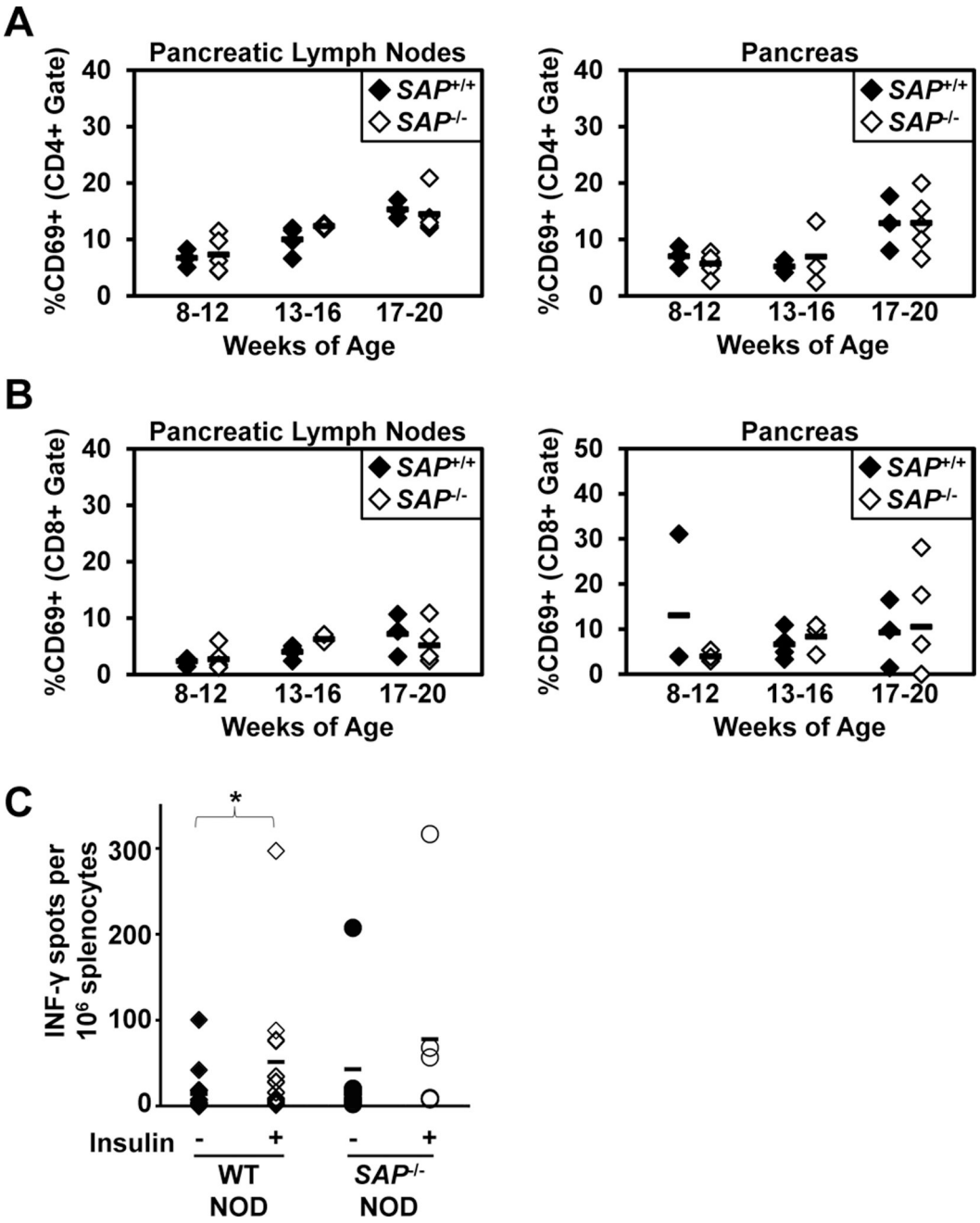

Figure 5. T cell activation and IFN-γ production is not blocked by loss of *SAP* in NOD mice.

(A-B) Pancreatic lymph nodes and pancreata were harvested from NOD (black) and *SAP*$^{-/-}$/NOD (white) pre-diabetic, female mice that were 8–12, 13–16, or 17–20 wks of age. Cells were gated on CD4^{+} (A) or CD8^{+} (B) live lymphocytes and the percentage of CD69^{+} cells was assessed in n ≥ 3 mice per group. No significant differences were observed between any of the age cohort comparisons of NOD vs. *SAP*$^{-/-}$/NOD mice using a two-tailed t test. (C) Splenocytes from female, pre-diabetic NOD mice (n=13) and *SAP*$^{-/-}$/NOD mice (n=6) were cultured in the presence or absence of 10μM insulin and IFN-γ production was measured by ELISpot. (C) The average number of IFN-γ secreting cells without

antigenic stimulation (black) and after stimulation (white) with insulin is shown for each mouse and the mean is indicated. Data are expressed as the average of technical triplicates of the number of spots /10^6 splenocytes). Each datapoint represents the mean response of an individual mouse. * $p < 0.05$, Mann-Whitney *U* test.

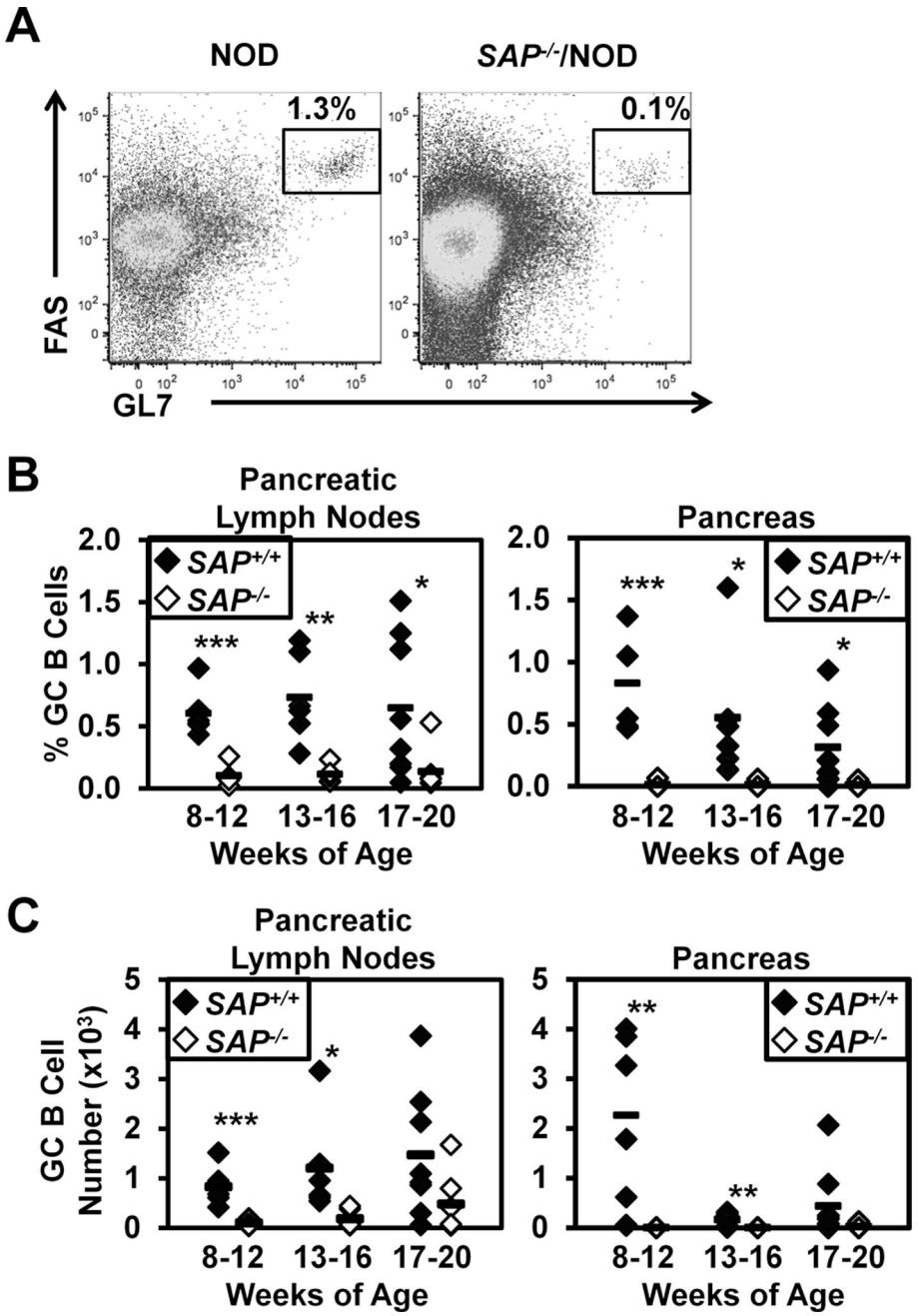

Figure 6. GC B cells are reduced in *SAP*$^{-/-}$/NOD mice.

Pancreatic lymph nodes and pancreata were harvested from NOD (black) and *SAP*$^{-/-}$/NOD (white) pre-diabetic, female mice. (A) Representative flow cytometry plots identify GC B cells (GL7^{high} FAS^{high}) among B220^{+} CD19^{+} live lymphocytes in lymph nodes. The frequency (B) or number (C) of GC B cells is shown for n ≥ 6 mice per group, n ≥ 3 experiments, * $p < 0.05$, ** $p < 0.01$, *** $p < 0.001$, two-tailed t test.

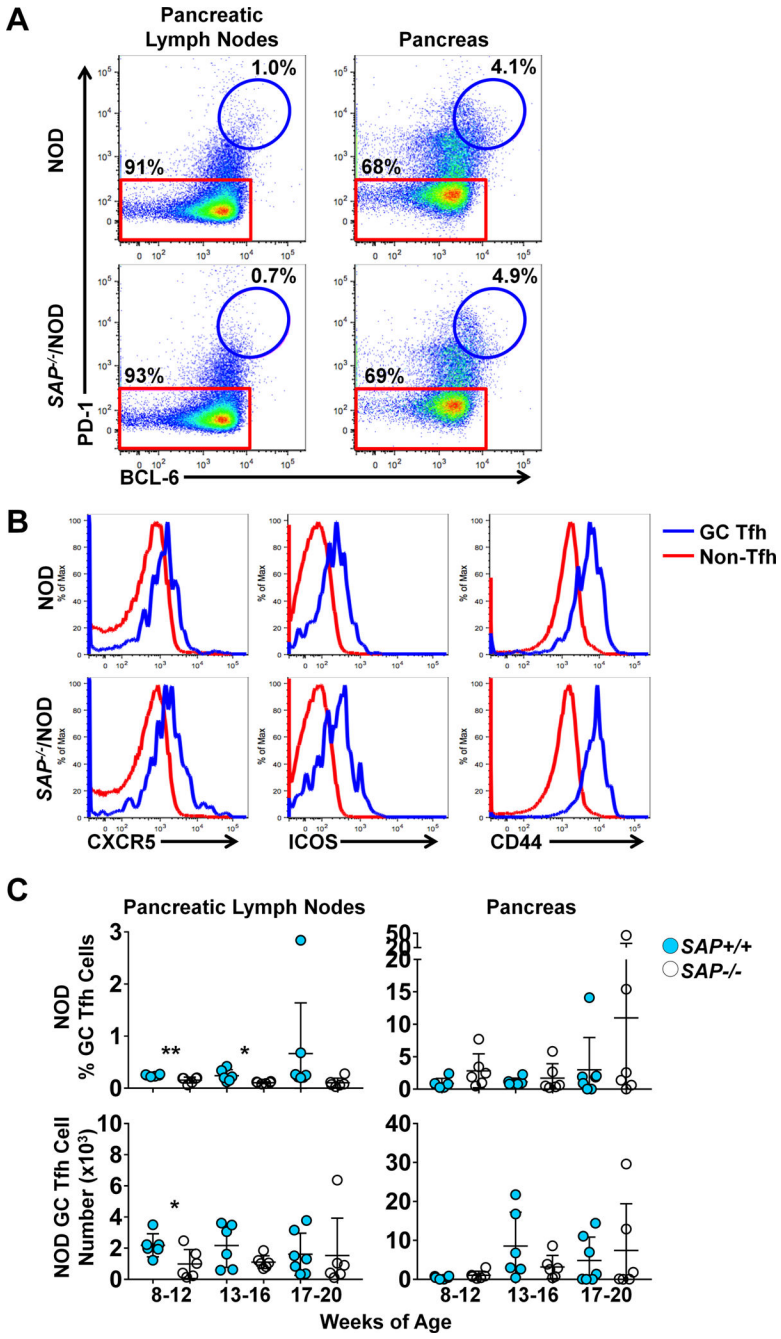

Figure 7. GC Tfh cells are present despite reduced GC B cells in *SAP*$^{-/-}$/NOD mice.

Pancreatic lymph nodes and pancreata were harvested from NOD (blue) and *SAP*$^{-/-}$/NOD (white) pre-diabetic, female mice. Cells were gated on CD4^{+} live lymphocytes. Non-Tfh cells (BCL-6^{low} PD-1^{low}, red), GC Tfh cells (BCL-6^{high} PD-1^{high}, blue) were identified using flow cytometry. (A) Representative plots are shown for pancreatic lymph nodes (left) or pancreas (right) harvested from NOD or *SAP*$^{-/-}$/NOD mice. (B) Histograms depict CXCR5, ICOS, and CD44 expression on Non-Tfh cells (red) and GC Tfh cells (blue) in pancreatic draining lymph nodes. (C) GC Tfh cell frequency (top) or number (bottom) is

shown for individual mice. n ≥ 6 mice per group, n ≥ 3 experiments, * $p < 0.05$, ** $p < 0.01$, *** $p < 0.001$, two-tailed t test.

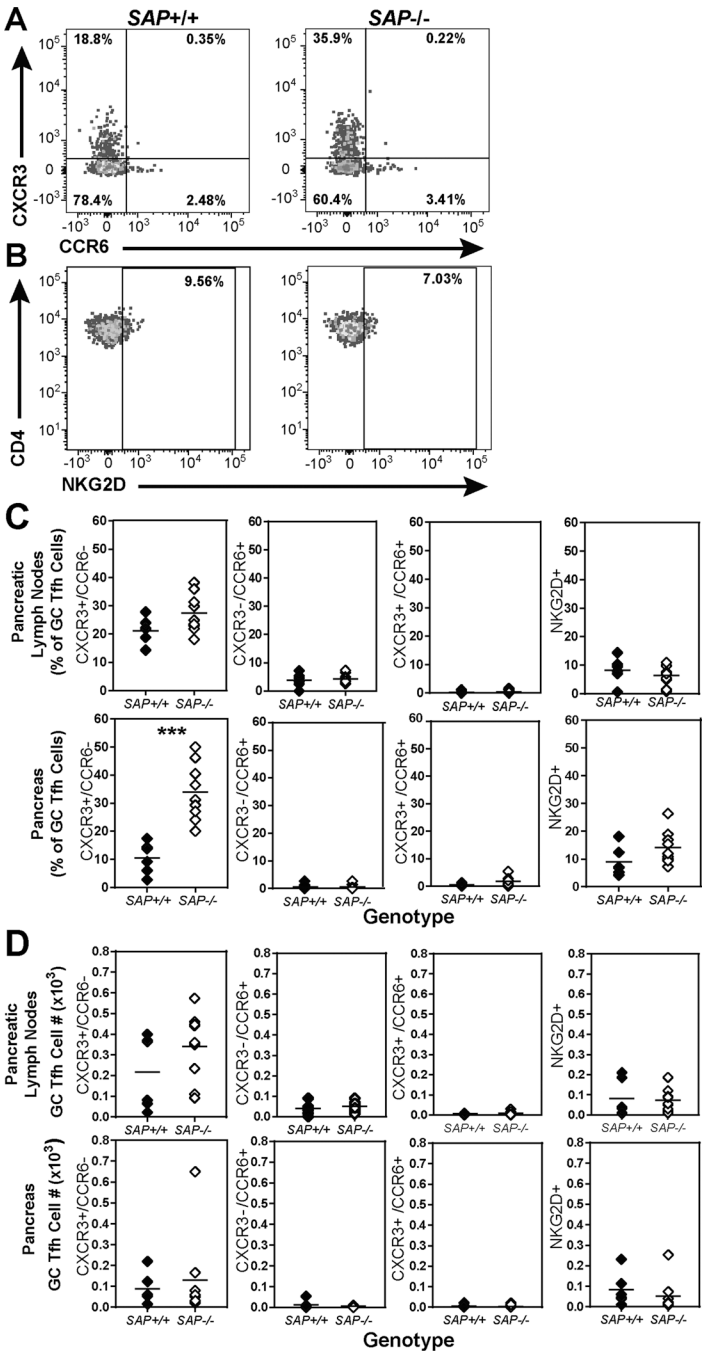

Figure 8. Tfh1 bias is enhanced by loss of *SAP* in the pancreas of NOD mice.

Pancreatic lymph nodes and pancreata were harvested from 15–23 wk-old $SAP^{+/+}$/NOD (black) and $SAP^{-/-}$/NOD (white) pre-diabetic, female mice. Cells were gated on $CD4^+$ $BCL6^+$ PD-1^{high} live lymphocytes (as in Fig. 7) and (A) $CXCR3^+$ $CCR6^-$ (Tfh1), $CXCR3^-$ $CCR6^-$ (Tfh2), $CXCR3^+$ $CCR6^+$ (Tfh17), and (B) $NKG2D^+$ subsets were identified by flow cytometry. Representative plots are shown for pancreatic lymph nodes harvested from $SAP^{+/+}$/NOD (left) or $SAP^{-/-}$/NOD (right) mice. (C-D) The frequency (C) and number (D) of Tfh1, Tfh2, Tfh17, and $NKG2D^+$ cells identified among GC Tfh cells as in Panels A-B is

shown for n ≥ 6 mice per group, n ≥ 3 experiments. Bars indicate the mean, *** $p < 0.001$, two-tailed t test.

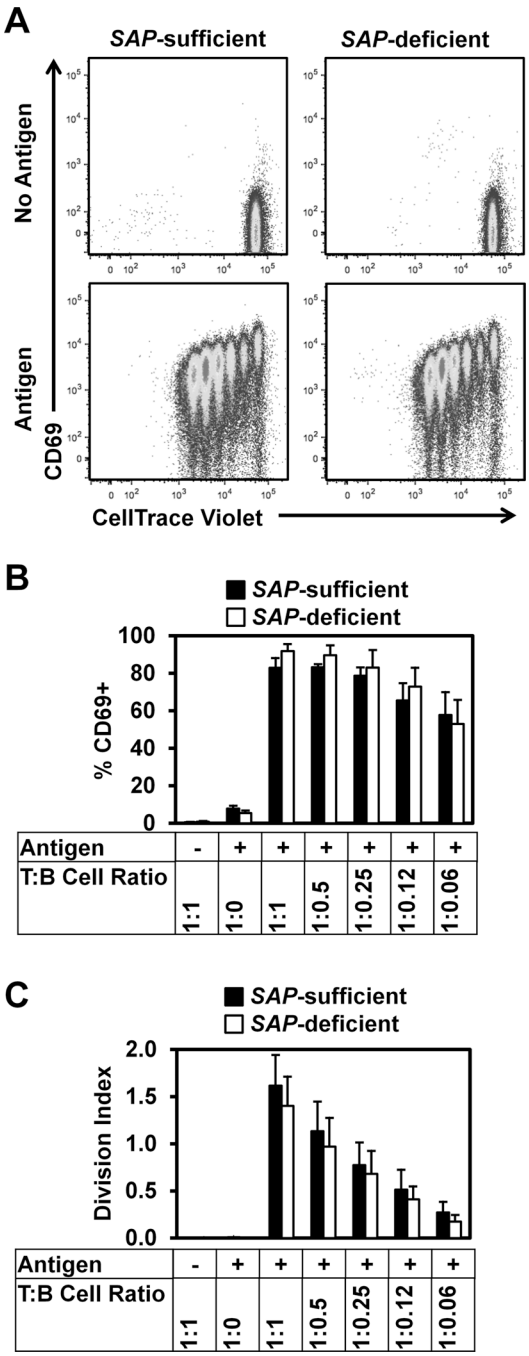

Figure 9. Loss of *SAP* does not impair proliferation of diabetogenic T cells in response to antigen presentation by B cells.

125Tg/NOD B cells and BDC2.5/NOD CD4$^+$ T cells (*SAP*-sufficient (black) or *SAP*-deficient (white) were MACS purified as in Methods. CD4$^+$ T cells were CellTrace Violet-labeled and co-cultured with the indicated ratio of 125Tg/NOD B cells +/− antigen (insulin-BDC mimotope) for 3 d. Activation and proliferation was measured among CD4$^+$ live lymphocytes using flow cytometry. (A) Representative plots of *SAP*-sufficient (left) or *SAP*-deficient (right) CD4 T cells co-cultured with B cells (1:1 ratio) with no antigen (top) or antigen (bottom). CD69$^+$ cell frequency (B), or the Division Index (C) of CD4$^+$ T cells) is

shown, n = 3 mice per group. All *SAP*-sufficient vs. *SAP*-deficient comparisons were not significant, two-tailed t test.

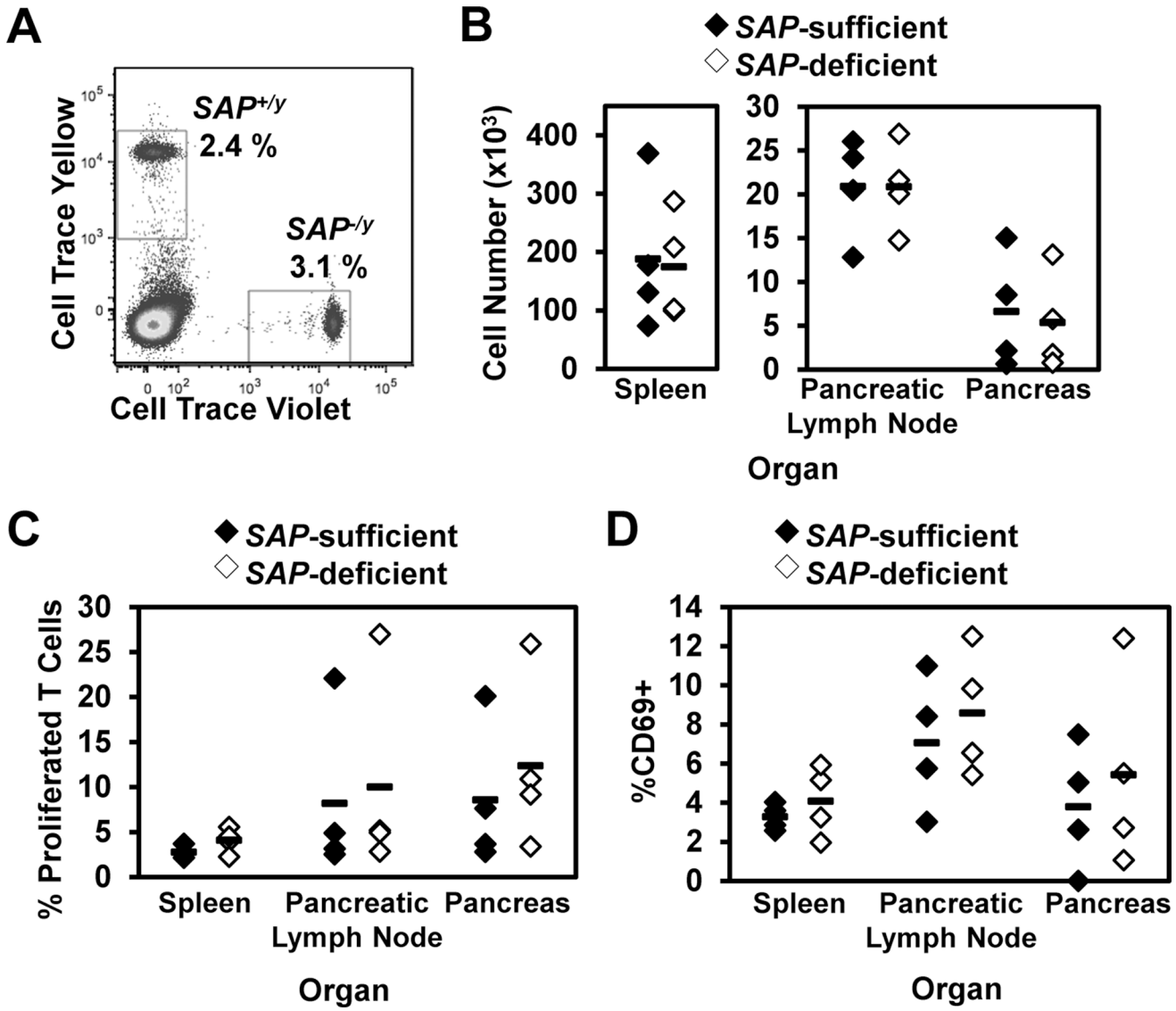

Figure 10. Loss of *SAP* does not limit proliferation of anti-insulin T cells *in vivo*.

MACS-purified 8F10/NOD (grey) or 8F10/*SAP*$^{-/y}$/NOD (white) CD4^{+} T cells were CellTrace Yellow or Violet-labeled. Equal numbers of *SAP*-sufficient and *SAP*-deficient cells (17–20×10^{6}) were mixed and injected i.p. into male VH125^{SD}/NOD recipients. After 1 wk, spleen, pancreatic lymph nodes, and pancreas were harvested. (A) Representative flow cytometry plots depict transferred cells among CD4^{+} live lymphocytes in lymph nodes. (B-D) The number of transferred T cells recovered from various organs (B), the percentage that underwent proliferation (C), and the frequency of CD69^{+} cells (D) is shown within live lymphocytes for individual mice. Averages are shown for n = 4 mice per group, all *SAP*-sufficient vs. *SAP*-deficient comparisons were not significant, two-tailed t test.